Monthly Notices
of the
ROYAL ASTRONOMICAL SOCIETY

MNRAS **444,** 2938–2959 (2014) doi:10.1093/mnras/stu1609

The influence of the environmental history on quenching star formation in a Λ cold dark matter universe

Michaela Hirschmann,[1,2★] Gabriella De Lucia,[1] Dave Wilman,[3] Simone Weinmann,[4] Angela Iovino,[5] Olga Cucciati,[6] Stefano Zibetti[7] and Álvaro Villalobos[1]

[1]*INAF – Astronomical Observatory of Trieste, via G.B. Tiepolo 11, I-34143 Trieste, Italy*
[2]*UPMC-CNRS, UMR7095, Institut d'Astrophysique de Paris, Boulevard Arago, F-75014 Paris, France*
[3]*Max-Planck-Institute for Extraterrestrial Physics, Giessenbachstrasse, D-85748 Garching, Germany*
[4]*Leiden Observatory, Leiden University, PO Box 9513, NL-2300 RA Leiden, the Netherlands*
[5]*INAF – Astronomical Observatory of Brera, via Brera 28, I-20159 Milano, Italy*
[6]*INAF – Astronomical Observatory of Bologna, via Ranzani 1, I-40127 Bologna, Italy*
[7]*INAF – Astrophysical Observatory of Arcetri, Largo Enrico Fermi 5, I-501125 Firenze, Italy*

Accepted 2014 August 6. Received 2014 August 6; in original form 2013 November 16

ABSTRACT

We present a detailed analysis of the influence of the environment and of the environmental history on quenching star formation in central and satellite galaxies in the local Universe. We take advantage of publicly available galaxy catalogues obtained from applying a galaxy formation model to the Millennium simulation. In addition to halo mass, we consider the local density of galaxies within various fixed scales. Comparing our model predictions to observational data [Sloan Digital Sky Survey (SDSS)], we demonstrate that the models are failing to reproduce the observed density dependence of the quiescent galaxy fraction in several aspects: for most of the stellar mass ranges and densities explored, models cannot reproduce the observed similar behaviour of centrals and satellites, they slightly underestimate the quiescent fraction of centrals and significantly overestimate that of satellites. We show that in the models, the density dependence of the quiescent central galaxies is caused by a fraction of 'backsplash' centrals which have been satellites in the past. The observed stronger density dependence on scales of 0.2–1 Mpc may, however, indicate additional environmental processes working on central galaxies. Turning to satellite galaxies, the density dependence of their quiescent fractions reflects a dependence on the time spent orbiting within a parent halo, correlating strongly with halo mass and distance from the halo centre. Comparisons with observational estimates suggest relatively long gas consumption time-scales of roughly 5 Gyr in low-mass satellite galaxies. The quenching time-scales decrease with increasing satellite stellar mass. Overall, a change in modelling both internal processes and environmental processes is required for improving currently used galaxy formation models.

Key words: methods: numerical – methods: observational – galaxies: evolution – galaxies: general – galaxies: formation – galaxies: statistics.

1 INTRODUCTION

It has long been known that the properties of galaxies are strongly dependent on the environment in which they are residing. Observations have revealed that red, early-type galaxies are preferentially located in high-density environments, while blue, late-type galaxies dominate the galaxy population in low-density environments (Oemler 1974; Davis & Geller 1976; Dressler 1980; Balogh et al. 1997; Poggianti et al. 1999). In the last decade, observational studies based on large spectroscopic and photometric surveys have invested significant effort to understand the role of environment on galaxy formation and evolution (e.g. Balogh et al. 2004; Kauffmann et al. 2004 and Blanton & Moustakas 2009 for a recent review). It remains, however, heavily debated to what extent the properties of galaxies are determined by external processes (nurture, i.e. interaction with other galaxies or with the local environment) or internal processes (nature, e.g. gas cooling, star formation, feedback processes, etc.).

In the nurture scenario, different environmental processes are thought to be effective in suppressing star formation and altering the morphology of a galaxy living in a 'dense' environment, such as strangulation (Larson, Tinsley & Caldwell 1980), ram-pressure

★E-mail: mhirsch@oats.inaf.it

© 2014 The Authors
Published by Oxford University Press on behalf of the Royal Astronomical Society

Downloaded from https://academic.oup.com/mnras/article/444/3/2938/1062092 by CNRS - ISTO user on 25 April 2022

stripping (Gunn & Gott 1972; Abadi, Moore & Bower 1999), tidal stripping (Dekel, Devor & Hetzroni 2003; Diemand, Kuhlen & Madau 2007) or harassment (Farouki & Shapiro 1981; Moore, Lake & Katz 1998). All these processes are expected to primarily affect *satellite* galaxies (i.e. galaxies orbiting within a halo containing a more dominant, *central* galaxy), and to have a stronger influence on those satellites residing in denser environments. However, their relative importance to quench star formation, as a function of density or halo mass, remains unclear.

Environmental effects might extend to central galaxies beyond the virial radius of a massive neighbour halo. Some observational studies (e.g. Balogh, Navarro & Morris 2000; Haines et al. 2009; von der Linden et al. 2010; Rasmussen et al. 2012; Geha et al. 2012) find an enhanced quiescent fraction of centrals in the vicinity of massive neighbour haloes out to four times the virial radius. Other studies find, however, no such trend. Environmental trends extending beyond the virial radius might – at least partly – be due to the fact that such galaxies have been residing inside a larger structure in the past. Balogh et al. (2000) first showed that in *N*-body simulations there are particles that have resided within the virial radius of clusters but have moved outside the virial radius later on. Present-day central galaxies could have behaved similarly as shown by Mamon et al. (2004) analytically or by e.g. Ludlow et al. (2009), Knebe et al. (2011) and Bahé et al. (2013) in numerical simulations. However, statistically, it remains unclear how strongly central galaxies are influenced by environmental effects. Thus, whether or not central galaxy properties depend on the environment on superhalo scales is currently heavily debated (see e.g. Blanton & Berlind 2007; Wilman, Zibetti & Budavári 2010; Peng et al. 2012; Bahé et al. 2013; Kovač 2014; Woo et al. 2013; Wetzel et al. 2014).

The effect of environmental processes has been theoretically studied by using semi-empirical models (Wetzel, Tinker & Conroy 2012), numerical simulations (see De Lucia 2011 for a review) and semi-analytic models (SAM; De Lucia & Blaizot 2007; Font et al. 2008; Kang & van den Bosch 2008; Kimm et al. 2009; Weinmann et al. 2010; Guo et al. 2011). Most of the currently used galaxy formation models do not explicitly include environmental processes beyond the virial radius of haloes. Environmental processes (working on satellites) are typically described by simplified recipes, e.g. an instantaneous strangulation of the hot halo gas of satellites. This leads to a significant overestimation of the quiescent fraction of model satellite galaxies compared to observations (e.g. Kimm et al. 2009). Some progress has been made by adopting a more gradual stripping of the hot gas associated with infalling galaxies (e.g. Font et al. 2008; Kang & van den Bosch 2008; Weinmann et al. 2010; Guo et al. 2011). The improved models are, however, still inconsistent with observations (e.g. with regard to the bimodality of the star formation rate distributions) indicating the need of further fundamental changes and modifications.

In the currently favoured hierarchical structure formation scenarios, based on the cold dark matter model (Peebles 1965; White & Rees 1978; Blumenthal et al. 1985), locally overdense regions collapse and form virialized dark matter haloes. Small objects form first and subsequently grow into larger systems via merging and smooth particle accretion. This implies that with evolving cosmic time, galaxies join more and more massive systems and therefore, experience a large variety of environments during their lifetime. In this context, external and internal effects are strongly connected and heavily intertwined, and disentangling the influence of nature and nurture is difficult.

A different evolution of galaxies in different environments is expected to leave an imprint on the observable galaxy properties. Haloes in overdense regions on average form earlier and merge more rapidly than those residing in regions of average density. In this respect, a detailed quantification of the influence of *the environmental history* on galaxy properties is still lacking, and appears to be of crucial importance in order to correctly explain and understand the observed environmental trends. A few recent studies have started to explore these issues such as Berrier et al. (2009), McGee et al. (2009), De Lucia et al. (2012), Hirschmann et al. (2013a) and Wetzel et al. (2013, 2014). Berrier et al. (2009) using numerical simulations and McGee et al. (2009) using SAM have studied the accretion history of galaxies on to clusters to investigate and to quantify the importance of pre-processing in galaxy groups. Hirschmann et al. (2013a) have investigated the environmental history of isolated galaxies in galaxy formation models and confirm that those are hardly affected by nurture and environmental effects during their lifetime.

Two recent studies of Wetzel et al. (2013, 2014) connect observational data with merger trees extracted from *N*-body simulations and adopt simple parametrizations for the evolution of star formation in satellites before and while their star formation is quenched. They predict long quenching time-scales for satellites and ejected centrals (up to 5 Gyr) increasing with decreasing stellar mass. Finally, a recent study by De Lucia et al. (2012) has focused on the environmental history of group and cluster galaxies. By comparing galaxy formation models to observational data, they also predict relatively long quenching time-scales of 5–7 Gyr within haloes more massive than $10^{13}\,M_{\odot}$, independent of the galaxy stellar mass. Their study treated the evolution as a function of estimated halo and stellar masses, but did not consider more detailed quantification of environment, such as the density of neighbouring galaxies on different scales. This partly motivates this work.

We present a detailed analysis of the effect of the environmental history by adopting similar approaches as in De Lucia et al. (2012). We take advantage of publicly available galaxy merger trees, obtained by applying the SAM of Guo et al. (2011) to the large cosmological dark matter Millennium simulation. The merger trees are analysed in order to study the history of the environment that galaxies have experienced during their lifetime, as a function of environmental density, stellar mass and galaxy type. In addition to estimated halo mass, we consider different density estimators that are commonly used in observational studies. For a comparison between model predictions and observations, we have computed densities based on the Sloan Digital Sky Survey (SDSS) DR8 data base (Wilman et al. 2010). In our analysis, we will particularly focus on the following points:

(1) First, we will specify the deficiencies of current galaxy formation models in predicting the observed environmental dependence of quiescent central and satellite galaxies.

(2) Secondly, we will explore the physical origin of the density dependence of quiescent central and satellite galaxies by considering their environmental history.

(3) Thirdly, we will discuss possible improvements for SAM by investigating the relevance of environmental processes on superhalo scales for quenching central galaxies and by constraining star formation quenching time-scales for satellite galaxies and their dependence on density and stellar mass.

The structure of the paper is as follows. In Section 2, we will briefly introduce the theoretical models and the observational data. In Section 3, we compare the stellar mass dependence of the quiescent fraction in observations and models. Section 4 presents a careful analysis of the density dependence of quiescent central

Downloaded from https://academic.oup.com/mnras/article/444/3/2938/1062092 by CNRS - ISTO user on 25 April 2022

and satellite galaxies and discusses the origin of these trends. In Section 5, we constrain quenching time-scales for satellite galaxies by considering their environmental history and comparing it with observational estimates. Finally, Section 6 gives a discussion and summary of this work.

2 METHOD

2.1 Observational data

We use observational data from the SDSS (DR8) data base which we cross-correlate with a modified catalogue of Wilman et al. (2010). This catalogue lists the neighbours of each galaxy within cylinders of different radii. Luminosities are computed using SDSS r-band Petrosian magnitudes, our adopted cosmology and k-corrected using the k-CORRECT IDL tool (Blanton & Roweis 2007). We select 'primary' galaxies with a SDSS r-band magnitude down to $M_r < -18$ at $z = 0$, but as 'neighbour' galaxies (galaxies used to calculate the density around a 'primary' galaxy) we take only galaxies brighter than $M_r < -20$. The galaxy sample is restricted to redshifts within the range $0.015 < z < 0.08$. This implies a volume-limited, and thus complete, 'neighbour' sample when assuming the magnitude cut of $M_r < -20$. Instead, the 'primary' galaxy sample with $M_r < -18$ is not volume limited over the full redshift range. Therefore, we limit our primary sample to smaller volumes for lower luminosity galaxies, and correct for volume incompleteness ($V_{\rm max}$ correction) throughout this study.

As a measure for environment, we consider the local densities of our 'primary' galaxies by calculating the projected surface density of neighbour galaxies, Σ_r, within a cylinder of depth $\pm 1000\,{\rm km\,s^{-1}}$ and with a projected radius centred on each primary galaxy, and selected to trace the environment on a scale of our choice. In this paper, we consider densities on two different scales, 1 and 0.2 Mpc. The former traces density on the scale of the most massive haloes at $z = 0$ while the latter examines the role of density on much smaller scales, but still large enough to avoid undersampling fairly dense environments with our luminosity limit. The projected surface density is then:

$$\Sigma_r = N_r/(\pi r^2), \quad (1)$$

where r is the radius of the cylinder and N_r is the number of neighbours corrected for spectroscopic completeness within this cylinder. Spectroscopic completeness of neighbours is evaluated and accounted for as described by Wilman et al. (2010). Within SDSS, correction factors are typically small, with a minority of large values in dense regions caused by fibre collisions. To ensure spectroscopic completeness corrections are feasible on scales up to 3 Mpc, we require high (>99.35 per cent, see Wilman et al. 2010) photometric completeness within this distance. This provides a total primary sample of 300 000 galaxies.

In order to additionally obtain specific star formation rates (sSFRs), stellar masses, halo masses and the central/satellite status for the observed galaxies, we have cross-correlated this catalogue with the corresponding catalogues from JHU-MPA[1] and the updated DR7 version of the group catalogue of Yang et al. (2007). The JHU-MPA DR7 catalogue is also updated with respect to the published DR4 version as described by Brinchmann et al. (2004, SFR) and Kauffmann (2003, stellar masses). These new catalogues contain not only a larger number of galaxies, but are also based on an improved methodology for the estimation of physical properties as described by Salim (2007). Spectral energy distribution (SED) fits to the photometry are used to improve stellar masses, aperture corrections to spectroscopically derived SFRs and the SFRs of galaxies where emission lines cannot be used. The group (or halo) catalogue employs an adaptive friends-of-friends (FOF) methodology with halo masses estimated using abundance matching and considering all galaxies brighter than an evolution and k-corrected r-band absolute magnitude of -19.5 (see Yang et al. 2007, for more details). 'Groups' can contain one or more galaxy, and a 'central' galaxy is simply identified as the most massive galaxy in each halo (in stars).

To select quiescent galaxies we use sSFR as a tracer, following Franx et al. (2008): quiescent galaxies have sSFR $= {\rm SFR}/M_{\rm star}$ smaller than $0.3 \times t_{\rm hubble}^{-1} \approx 10^{-11}\,{\rm yr^{-1}}$. It is important that we define quenching by low SFR rather than by red colour, given that one-third of the red galaxies are star forming and the results are sensitive to this choice as was shown by Woo et al. (2013).

2.2 The galaxy formation model

2.2.1 *Millennium simulation and cosmology*

To compare observed galaxies with model predictions, we take advantage of the publicly available catalogues from the galaxy formation model presented by Guo et al. (2011). This model was applied to the dark matter merger trees extracted from the Millennium simulation (Springel 2005). The simulation assumes a *WMAP*1 cosmology with $\Omega_\Lambda = 0.75$, $\Omega_{\rm m} = 0.25$, $\Omega_{\rm b} = 0.045$, $n = 1$, $\sigma_8 = 0.9$ and, $h = 0.73$. Note that more recent measurements of the CMB e.g. with the *Planck* satellite (Planck Collaboration XVI 2013) obtain a slightly smaller value for $\sigma_8 = 0.83$. If only σ_8 is changed, the present-day Universe corresponding to a σ_8 lower than that used in our simulation can be well approximated by a snapshot corresponding to some earlier redshift (see e.g. Wang et al. 2008). The quantitative results presented in the following (e.g. the fraction of quiescent central and satellite galaxies) would slightly change. However, we do not expect the qualitative trends discussed below to be altered significantly.

2.2.2 *Environmental processes in the SAM*

The galaxy formation model of Guo et al. (2011) includes prescriptions for gas cooling, reionization, star formation, supernova feedback, metal evolution, black hole growth and AGN feedback. This model is based on the earlier models by De Lucia & Blaizot (2007) and Croton (2006) but adopts a modified treatment of environmental processes acting on satellite galaxies (strangulation, ram-pressure and stellar stripping) and of supernova feedback. In addition, the Guo model assumes that galaxies effectively become satellites only when they fall within $r_{\rm vir}$ and not – as in the earlier models – as soon as they belong to a larger FOF group implying that environmental effects start influencing galaxies at a later time. This definition for a satellite galaxy is applied to both type-1 (having a dark matter subhalo) and type-2 satellites (orphan galaxies). Furthermore, the hot gas mass associated with galaxies being accreted on to larger structures is assumed to be reduced by tidal stripping in direct proportion to the subhalo's dark matter mass (followed directly in the simulations). In addition to tidal forces, the hot gas around satellite galaxies is assumed to experience ram-pressure forces due to the motion of a satellite galaxy through the intercluster medium. At the radius where the ram pressure is dominating over the self-gravity (to bind the gas), the hot gas is completely stripped. The

[1] http://www.mpa-garching.mpg.de/SDSS/DR7/

Downloaded from https://academic.oup.com/mnras/article/444/3/2938/1062092 by CNRS - ISTO user on 25 April 2022

stripping of the hot gas is less efficient than in the model of De Lucia & Blaizot (2007), who assumed an instantaneous stripping of the hot gas. For more details, we refer the reader to Guo et al. (2011).

2.2.3 *Limitations of the SAM and other models*

The model has been shown to reproduce qualitatively a large variety of data, both at high redshift and in the local Universe. However, it is not without problems: even if the model can reproduce the present-day stellar mass function due to a stronger supernova feedback than in former models, it still overpredicts low-mass galaxies at higher redshifts. In addition, the predicted fraction of red (satellite) galaxies is still too high with respect to observational measurements.

These drawbacks are not specific to this particular galaxy formation model, and rather represent one of the major challenges for recently published SAM (e.g. Bower et al. 2006, Somerville et al. 2008, Bower, Benson & Crain 2012, Hirschmann et al. 2012a,b; Weinmann et al. 2012), as well as for hydrodynamic simulations (Davé, Oppenheimer & Finlator 2011; Weinmann et al. 2012; Hirschmann et al. 2013b). There have been some recent attempts to solve these problems by changing the star formation prescription (Wang, Weinmann & Neistein 2012) or by adopting reincorporation time-scales which vary inversely with halo mass (Henriques et al. 2013), but none of the proposed solution has been shown to be completely satisfactory and successful.

2.2.4 *Mimicking observations with the SAM*

To perform a fair comparison between observations and model predictions, we have projected the cosmological box along the z-axis. As in the observations, we use the sSFR as a tracer for the quiescence of a galaxy. When looking at the distributions of sSFRs at a given stellar mass and 1 Mpc density, we find that the adopted cut (10^{-11} yr^{-1}) provides a suitable selection criterion for quiescent galaxies for both models and observations.

As a measure for environment, we consider the theoretical halo mass and the local densities of the model galaxies. For the latter, we compute the projected density within a cylinder considering two different radii, $r = 0.2$ Mpc and $r = 1$ Mpc using equation (1).

To be consistent with the observations, we adopt the same luminosity cuts in the models: we consider as 'primary' galaxies those with an SDSS r-band magnitude down to $M_r < -18$ at $z = 0$, and as 'neighbour' galaxies only those brighter than $M_r < -20$ within $\Delta v = \pm 1000$ km s^{-1} of the 'primary' galaxy (taking into account the peculiar velocities of the neighbour galaxies). To assess the environmental histories of our model galaxies, we will make use of the galaxy merger trees, but consider only the main branch of the trees, i.e. the main progenitors of the $z = 0$-galaxies (see fig. 1 in De Lucia et al. 2012).

2.3 Misclassification of centrals and satellites

The distinction between central and satellite galaxies in the models is based on the dynamical and positional information coming from the simulations: by construction, central galaxies are those sitting at the centre of FOF groups, and satellites are all other galaxies gravitationally bound to the same FOF. In the observations, the central/satellite classification is obtained from the group catalogue by Yang et al. (2007). As summarized in Section 2.1, this is built by running an FOF algorithm on the data, and then assigning a central/satellite status according to a simple mass rank.

Before comparing the observed quiescent central and satellite fractions to model predictions, we quantify the contamination fractions due to the group classification algorithm used for the data. To this aim, we have employed a central/satellite catalogue obtained by applying the Yang et al. (2007) algorithm for groups detection and satellite/central classification to the galaxies of the Guo model. Fig. 1 shows the fractions of misclassified centrals (yellow-dashed) and satellites (green-solid) at a given stellar mass, as a function of the 1Mpc-density. We have also specified the total contamination fraction in each mass bin (see legend). The contamination of the satellite sample is due to misclassified central galaxies as group members, which may happen if they reside in the vicinity of a group. Instead, contamination of the central sample occurs when the group finder incidentally breaks up one group into smaller ones. We find no strong dependence of the contamination fractions on density (even if for low-mass satellites the contamination fractions tend to decline with increasing density). At a given stellar mass bin, the fractions are significantly lower than 10 per cent for both centrals and satellites (except for low-mass satellites).

Following the approach adopted by Weinmann et al. (2009), we use these contamination fractions to estimate the uncontaminated quiescent fractions for both centrals and satellites. Briefly, using the contamination fractions at a given density and stellar mass $c_{\rm sat/cent}$, and given some observational average quantity $\hat{p}_{\rm sat}$ and $\hat{p}_{\rm cen}$, one can estimate the corresponding uncontaminated average quantities $\bar{p}_{\rm sat}$ and $\bar{p}_{\rm cen}$ from

$$\hat{p}_{\rm sat} = (1 - c_{\rm sat})\bar{p}_{\rm sat} + c_{\rm sat}\bar{p}_{\rm cen} \quad (2)$$

$$\hat{p}_{\rm cen} = c_{\rm cen}\bar{p}_{\rm sat} + (1 - c_{\rm cen})\bar{p}_{\rm cen}. \quad (3)$$

We find that the quiescent fractions (at a given stellar mass and density) remain almost unchanged. Thus, in the following analysis, we present results uncorrected for contamination.

3 THE STELLAR MASS DEPENDENCE OF QUIESCENT GALAXIES

The quiescent fraction of galaxies is known to be dependent on both stellar mass and density. The dependence on density is strongest for quiescent low-mass galaxies (see e.g. Peng et al. 2012). In Fig. 2, we start by investigating the stellar mass dependence of the quiescent fraction of all (red-dotted), central (yellow-dashed) and satellite (green-solid) galaxies in the Guo model (lines) and in the observations (symbols). The quiescent fractions $f_{\rm quiescent}$ have been calculated as

$$f_{\rm quiescent} = n_{\rm qu,x}/n_{\rm x}, \quad (4)$$

where x indicates the (sub-)population of galaxies (all, centrals, satellites), $n_{\rm qu,x}$ is the number of quiescent galaxies and $n_{\rm x}$ the total number of these galaxies. The error bars in these plots are 68 per cent confidence limits from the Wilson (1927) binomial confidence interval (this is the case for all the following figures, unless otherwise stated).

Comparing the observations to the results of Kimm et al. (2009, not shown in Fig. 2), our observed, quiescent fractions at galaxy masses below $\log(M_{\rm stellar}/{\rm M}_\odot) < 10$ are somewhat lower than theirs, particularly for satellite galaxies. Kimm et al. (2009) use the Yang catalogue based on the SDSS data similar to our analysis, adopt the same magnitude cut and perform a completeness correction. However, they use SFR estimates based on full SED modelling, while Brinchmann et al. (2004) – as used in our analysis – have estimated the SFR via emission lines. It seems likely

Downloaded from https://academic.oup.com/mnras/article/444/3/2938/1062092 by CNRS - ISTO user on 25 April 2022

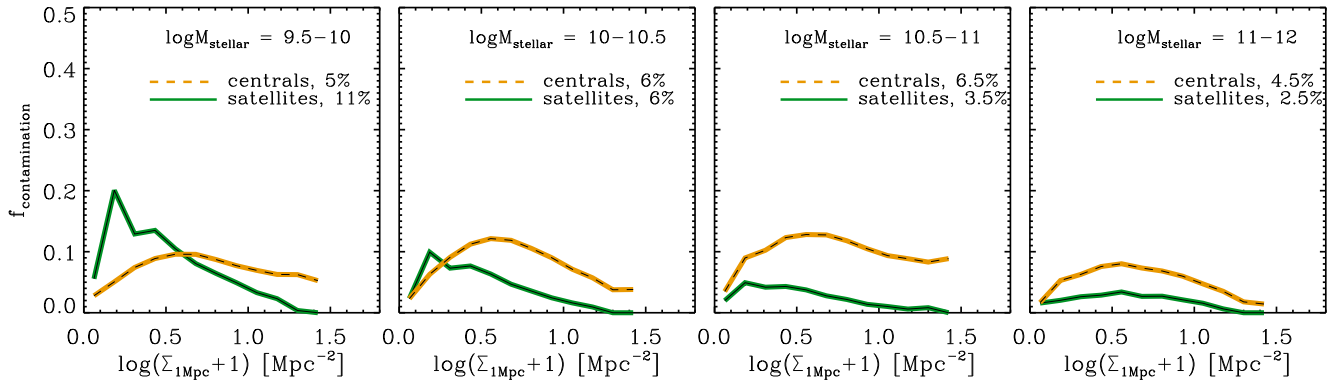


Figure 1. The fraction of central (yellow-dashed) and satellite (green-solid) galaxies that are misclassified by the algorithm used for the data. These are computed by applying the same method used for the observed group catalogue (Yang et al. 2007) to a mock catalogue built from the Guo et al. (2011) model. Contamination fractions are shown at given stellar masses and as a function of the 1 Mpc density. Except for the low-mass satellite galaxies, contamination fractions are always below 10 per cent.

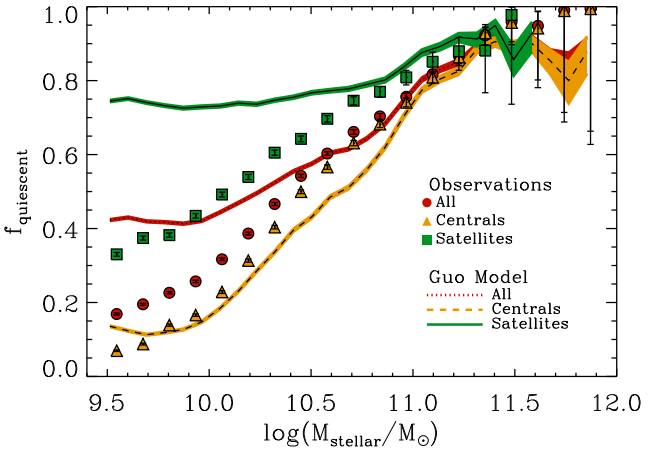


Figure 2. Quiescent fraction of all (red-dotted), central (yellow-dashed) and satellite (green-solid) galaxies versus the galaxy stellar mass for the Guo model (lines and shaded areas) and observations (symbols). At fixed stellar mass the quiescent central fraction in the models is partly slightly underpredicted, while the amount of quiescent satellites is significantly overpredicted.

that part of the discrepancy relates to the detection threshold in UV driving an SFR limit which increases to higher sSFR for lower mass galaxies. There is a population of galaxies which has sSFR $<10^{-11}$ for the SED fitting including UV, but sSFR $>10^{-11}$ according to Brinchmann et al. (2004).

Turning to the model predictions, at galaxy masses below $\log(M_{\rm stellar}/{\rm M}_\odot) < 10.5$, the predictions of the Guo model significantly overestimate the observed, quiescent satellite fraction, while they slightly underestimate the central one at intermediate stellar masses. This indicates that the treatment of central galaxies in the models also needs to be revised. In addition, this demonstrates that even the more relaxed, delayed strangulation assumption in the Guo model (compared to the instantaneous strangulation) is not sufficient to solve the well-known 'overquenching problem' of satellite galaxies with masses below $\log(M_{\rm stellar}/{\rm M}_\odot) < 10.5$. Overall it shows, that the recipes for the physical processes working on both satellite and central galaxies need to be further refined.

4 THE DEPENDENCE OF QUIESCENT GALAXIES ON THEIR ENVIRONMENT

4.1 The fraction of quiescent galaxies as a function of density

In this section, we investigate how model predictions of quiescent fractions as a function of environment deviate from observations. We consider the importance of halo mass, central versus satellite status, and the projected density within a 1 and a 0.2 Mpc cylinder (as explained in Section 2).

Fig. 3 shows the quiescent fraction of all (red-dotted), central (yellow-dashed) and satellite (green-solid) galaxies versus the 1 Mpc density (top row) and versus the 0.2 Mpc density (bottom row) for the Guo model (lines) and the observations (symbols). We have divided our central and satellite sample into different stellar mass bins (as indicated in the legend) in order to separate the dependence of the quiescent fraction on stellar mass and on density.

It is remarkable that in the observations, quiescent fractions at a given stellar mass and density are very similar for satellite and central galaxies, and that both fractions reveal a strong dependence on density for stellar masses below $\log(M_{\rm stellar}/{\rm M}_\odot) < 10.5$.

In contrast to the observations, the modelled quiescent fractions reveal significantly larger differences between satellites and centrals. For satellites, the agreement between observations and model predictions is reasonably good for massive galaxies ($\log(M_{\rm stellar}/{\rm M}_\odot) > 10.5$) and for those in high-density regions ($\log(\Sigma_{\rm 1Mpc} + 1) > 1[{\rm Mpc}^{-2}]$). Apart from that, at a given density and stellar mass below $\log(M_{\rm stellar}/{\rm M}_\odot) < 10.5$, the Guo model significantly overpredicts the fraction of quiescent satellites. The disagreement gets worse with decreasing galaxy mass and decreasing density. In addition, for satellites with stellar masses below $\log(M_{\rm stellar}/{\rm M}_\odot) < 10.5$ the model predicts a weaker dependence on both the 0.2 Mpc and the 1 Mpc density than what is observed.

For centrals, the dependence of the quiescent fraction on the 1 Mpc density is weaker in the models than in the observations, while the dependence on the 0.2 Mpc density has similar strength. The model also predicts realistic quiescent central fractions at high stellar masses $\log(M_{\rm stellar}/{\rm M}_\odot) > 11$ or at very low densities. Otherwise, at higher densities and for lower stellar masses, the Guo model underestimates the amount of quiescent centrals: the mismatch becomes stronger for centrals with decreasing galaxy masses and increasing densities.

Downloaded from https://academic.oup.com/mnras/article/444/3/2938/1062092 by CNRS - ISTO user on 25 April 2022

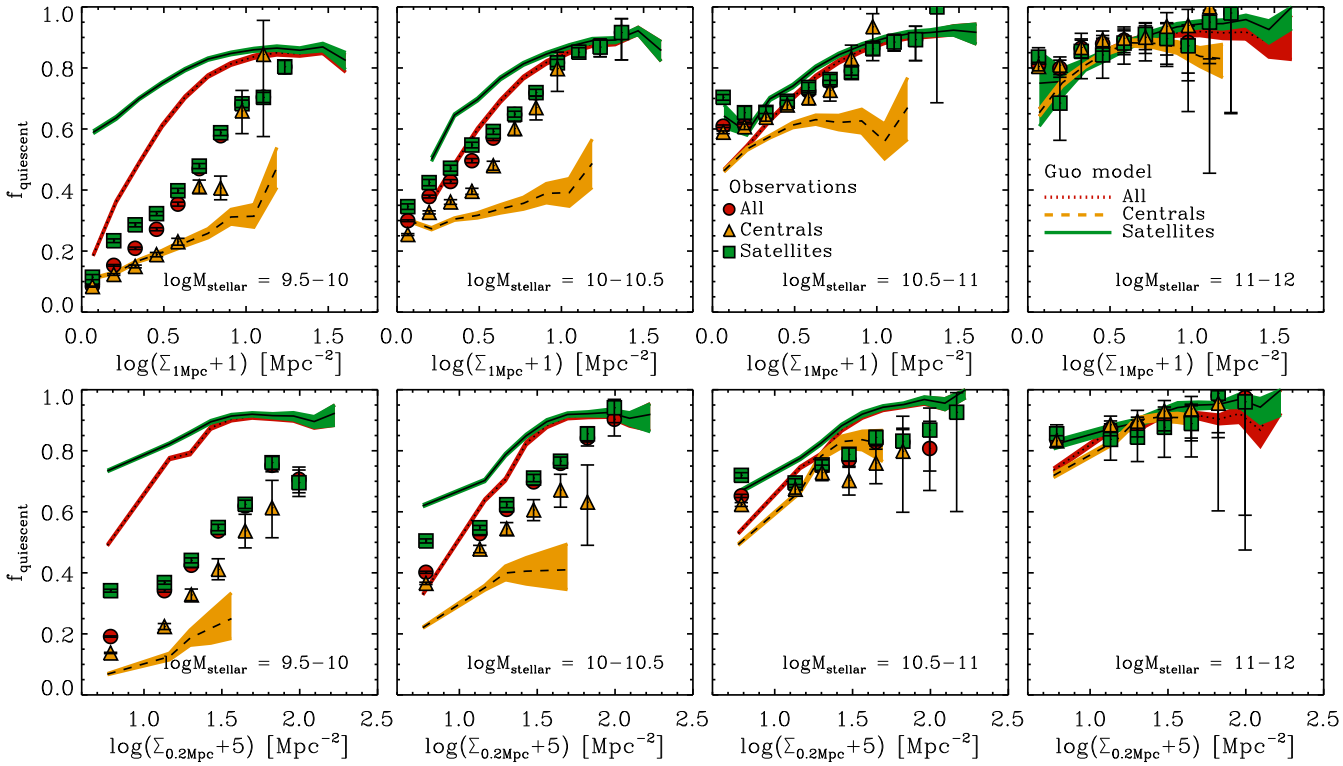


Figure 3. Quiescent fraction of all (red-dotted), central (yellow-dashed) and satellite (green-solid) galaxies versus the projected density of a 1 Mpc cylinder (top row) and of a 0.2 Mpc cylinder (bottom row) for the observations (symbols) and for the Guo model (lines). Different columns correspond to different stellar mass bins as indicated in the legend. At stellar masses below 3×10^{10} $M_{\odot}$, observations show a strong correlation between the quiescent fraction and density of both satellites and centrals. For stellar masses above 10^{10} $M_{\odot}$, there is only very weak difference between observed centrals and satellites which is insignificant contrast to the model predictions.

We find that the offset between model predictions and observations at fixed density is driven by the contribution of haloes with mass $\log(M_{\rm halo}/M_{\odot}) < 11.7$, where the fraction of quiescent model centrals is very low (it rapidly increases for more massive haloes). Since these low-mass haloes are close to the resolution limit of the Millennium simulation, we have tested and confirmed that model quiescent fractions are not affected by resolution using the Guo model applied to the Millennium-II simulation (this corresponds to a smaller cosmological volume, but a higher resolution). The disagreement found indicates that also the treatment of model central galaxies needs to be improved (this is in agreement with previous studies, see e.g. Cucciati et al. 2012).

Comparing the 1 Mpc density with the smaller scale 0.2 Mpc density in observations, for both the central and satellite quiescent fractions with stellar masses below $\log(M_{\rm stellar}/M_{\odot}) < 11$, the dependence on the 0.2 Mpc density is slightly weaker than the one on the 1 Mpc density (the relative increment of the quiescent satellite fractions from low density to high density, $=f_{\rm qu,sat}(\text{high }\Sigma)/f_{\rm qu,sat}(\text{low }\Sigma)$ is larger for the 1 Mpc than for the 0.2 Mpc density). Also model quiescent satellites show a slightly weaker dependence on the 0.2 Mpc density than on the 1 Mpc one (this will be discussed further in Section 4.3).

To understand how important the environmental dependence is in the population of central galaxies, Fig. 4 shows the distributions of central (yellow) and satellite (green) galaxies (normalized to the total number of centrals and satellites in each mass bin) as a function of the 1 Mpc density for different stellar mass bins (different panels). Data are shown as symbols, while model predictions are shown by solid lines. The agreement between model predictions and observations is generally very good, particularly for the lowest stellar mass bin considered, even if for the more massive galaxies, models overpredict the number of satellites at $\log(\Sigma_{\rm 1Mpc}+1) > 3.0$ and they overpredict the fraction of massive centrals at all densities by a factor 2. The fractions of central galaxies residing at densities $\log(\Sigma_{\rm 1Mpc}+1) > 0.3$ vary between 15 and 25 per cent in the data (the largest fractions are found in the highest stellar mass bin) and between 12 and 50 per cent in the models. The bulk of central galaxies is residing at low densities, while satellite galaxies dominate the high-density regions. Therefore, the density dependence of the overall galaxy population is driven by satellite galaxies. There is, however, a non-negligible fraction of central galaxies residing in high-density regions, and their quiescent fractions increases with increasing density.

4.2 Relation between density and halo mass

In this section, we explore the *theoretical* interpretation of the observed density dependence (particularly on the 1 Mpc density) of both centrals and satellites. We start by investigating whether the density dependence reflects a dependence on halo mass, i.e. we analyse whether and how strongly the 1 Mpc and the 0.2 Mpc density is related to the halo mass of centrals and the parent halo mass of satellites.

Fig. 5 shows the median halo mass versus the 1 Mpc density (top row) and versus the 0.2 Mpc density (bottom row) for centrals (yellow-dashed) and satellites (green-solid) in models (lines) and observations (symbols). The shaded areas indicate the range between the 25th and 75th percentile of the distribution of halo

Downloaded from https://academic.oup.com/mnras/article/444/3/2938/1062092 by CNRS - ISTO user on 25 April 2022

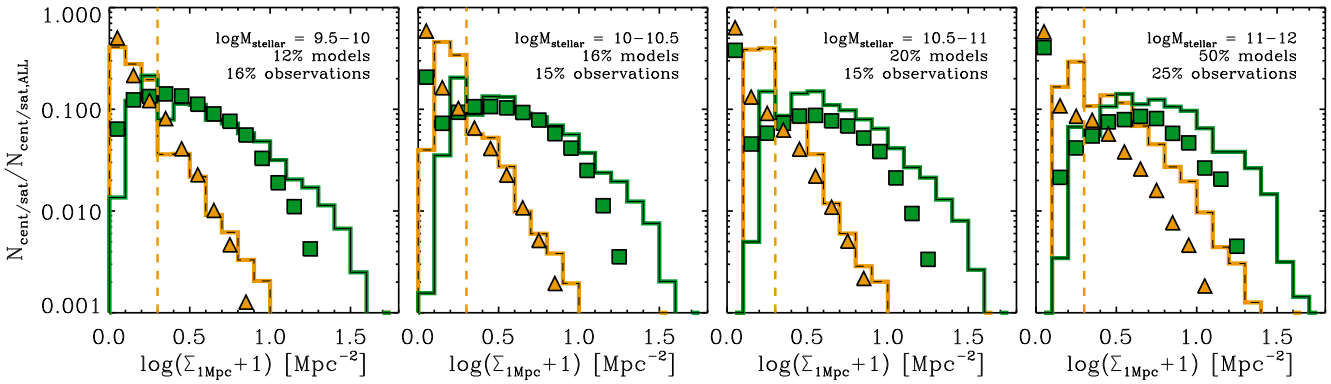


Figure 4. Distribution of central (yellow-dashed) and satellite (green-solid) galaxies (fractions are normalized to the total number of centrals and satellites in each mass bin considered) as a function of the 1 Mpc density for different bins of stellar mass. Model predictions are shown as solid lines, while observational data are shown as symbols. The agreement between models and observations is very good. The fractions given in each panel correspond to the fractions of central galaxies in models and observations living at densities above $\log(\Sigma_{1\,\mathrm{Mpc}}+1)=0.3$ (as indicated by the vertical dashed line), where data show a strong density dependence for quiescent centrals (see Fig. 3).

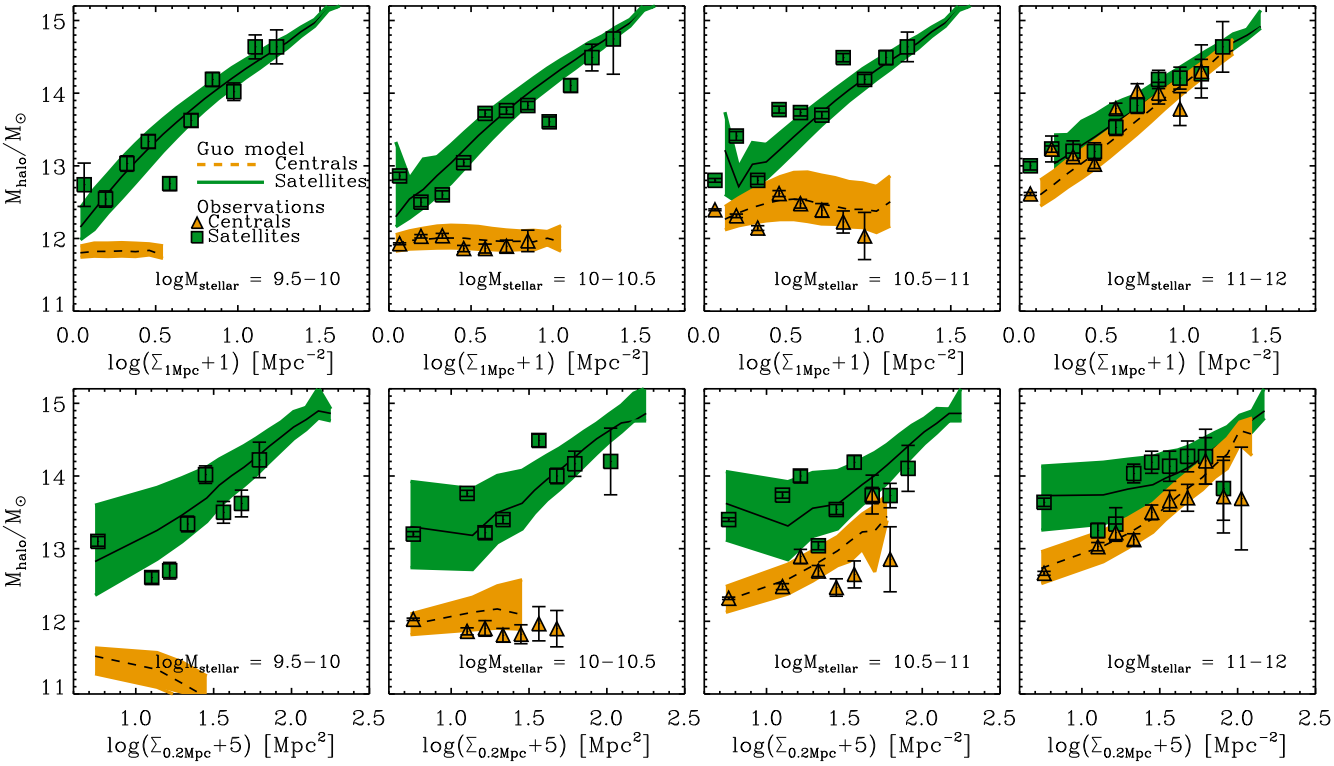


Figure 5. Median parent halo mass versus the 1 Mpc density (top row) and versus the 0.2 Mpc density (bottom row) in different stellar mass bins (different columns) for the Guo model (shaded areas) and for the observations (symbols). We also distinguish between satellites (green areas, solid lines and squares) and centrals (yellow areas, dashed lines and triangles). The shaded areas and the error bars of the symbols refer to the 25th and 75th percentiles, respectively. Observations and models are in good agreement: the parent halo mass of satellites scales with their density, but interestingly, the halo mass of centrals correlates with density only for the most massive galaxies (right-hand column).

masses at fixed density. For both centrals and satellites, we find good agreement between models and observations. This analysis extends a recent study of Haas, Schaye & Jeeson-Daniel (2012), who also investigate the relation between density (using different estimators) and halo mass (see also Muldrew (2012)), but they do not distinguish between centrals and satellites or different stellar mass bins. They find that the density (for fixed aperture densities) is *always* correlated with halo mass.

Our results are consistent with theirs when we consider satellite galaxies: the parent halo mass of satellites is strongly correlated with density irrespective of the density scale and the stellar mass. The median parent halo masses are above $\log(M_{\mathrm{halo}}/\mathrm{M}_\odot)=12.5$ corresponding to virial radii larger than >0.2 Mpc.

The correlation between parent halo mass and density is slightly weaker for the 0.2 Mpc scale than for the 1 Mpc scale (the median parent halo masses at low 0.2 Mpc densities are higher than at low 1 Mpc densities). This is likely due to the fact that the small-scale 0.2 Mpc density preferentially traces 'intrahalo' scales (i.e. scales smaller than the virial radius) of parent haloes more massive than $\log(M_{\mathrm{halo}}/\mathrm{M}_\odot) > 12.5$. In contrast, the 1 Mpc density will capture the entire haloes up to masses of $\log(M_{\mathrm{halo}}/\mathrm{M}_\odot)=15$ corresponding to virial radii of roughly 1 Mpc.

Downloaded from https://academic.oup.com/mnras/article/444/3/2938/1062092 by CNRS - ISTO user on 25 April 2022

This behaviour explains some of the trends shown in Fig. 3, where the dependence of the quiescent satellite fraction on the 0.2 Mpc density was shown to be slightly weaker than the one on the 1 Mpc density. This indicates that densities of intrahalo scales do not capture the total effect of environment on quiescent satellites.

In contrast to the satellites, the halo mass of central galaxies (yellow areas in Fig. 5) depends on the 1 Mpc density (resp. the 0.2 Mpc density) only for massive galaxies with $\log(M_{\rm stellar}/{\rm M}_\odot) > 11$ (resp. $\log(M_{\rm stellar}/{\rm M}_\odot) > 10.5$). In other words, a correlation between the 1 Mpc density (resp. 0.2 Mpc density) and halo mass only emerges for galaxies with a median halo mass above $\log(M_{\rm halo}/{\rm M}_\odot) \sim 13$ (resp. $\log(M_{\rm halo}/{\rm M}_\odot) \sim 12.5$). Such halo masses correspond roughly to virial radii larger than ∼300 kpc (resp. ∼200 kpc). This means that the 1 Mpc density probes *superhalo scales* for haloes with $\log(M_{\rm halo}/{\rm M}_\odot) \sim 13$. For smaller haloes (in which low-mass centrals are preferentially sitting, $\log(M_{\rm halo}/{\rm M}_\odot) \sim 11-12$ with $r_{\rm vir} \leq 150$ kpc), 1 and 0.2 Mpc densities do not correlate with the halo masses, neither in models nor in observations. This reflects the averaging over scales larger than the corresponding virial radii.

To summarize this section, the strong correlation between density and host halo mass for satellites implies that the dependence of the quiescent satellite fractions on the 1 Mpc density (see the top row of Fig. 3) can be theoretically understood – at least partly – in terms of their dependence on parent halo mass. However, the correlation between density and halo mass does not allow for any conclusion about the fundamental relation between environment and the quiescent fraction. We will discuss this in more detail in Section 4.4. In contrast, given that density and halo mass are unrelated for centrals (Fig. 5), the density dependence of quiescent central fractions, particularly those of lower mass galaxies, can hardly originate from a dependence on halo mass.

4.3 Central galaxies

We have shown in Section 4.2 that the halo mass of centrals can hardly be responsible for the density dependence of low-mass quiescent centrals. This result may indicate the existence of environmental effects on superhalo scales affecting central galaxies. There are two possible explanations for this.

First, present-day central galaxies may have been satellites in the past and therefore, they can have experienced environmental processes like strangulation for some fraction of their lifetime. Such satellites have probably been on highly eccentric orbits so that – after one or more pericentre passages – they could have left their parent halo and become central galaxies again (outside the virial radius of the previous parent halo). We refer to these present-day central galaxies as 'backsplash' centrals. Strictly speaking, of course, such backsplash centrals are not affected by environment of superhalo scales but have been subject to environmental effects while orbiting within a more massive halo in the past.

The galaxy formation model accounts for such a backsplash effect automatically as it uses the kinematic input from dark matter simulations (i.e. it follows the orbits from the simulations): as long as the backsplash central galaxy is a satellite, it is assumed to be affected by tidal and ram-pressure stripping. After ejection from the parent halo, the backsplash central is treated as a 'normal' central galaxy which means that such a galaxy does not experience any environmental effects anymore. Instead, it can (re-)accrete gas which can cool and form stars. Nevertheless, its hot halo content is reduced due to the time spent as satellite and thus, a backsplash central galaxy evolves differently to if it had always been a central galaxy in the past.

Alternatively, central galaxies, which have never been satellites in the past, might suffer environmental effects on superhalo scales. This was nicely demonstrated in recent study of Bahé et al. (2013) using hydrodynamical simulations. They found that a direct interaction with an extended hot gas 'halo' of a group or cluster can be sufficiently strong to strip the hot gas atmospheres of infalling galaxies as far out as $\sim 5 \times r_{\rm vir}$. However, the hot gas stripping was not found to significantly affect the ongoing star formation and the quiescent fraction of galaxies outside the virial radius. It may, thus, be expected to have only a minor impact. So far, there is no recipe in the models to account for this second effect.

4.3.1 *Backsplash population*

To quantify the statistical relevance of the backsplash population in the models (note that this information is of course not accessible in the observations), we make use of the galaxy merger trees of the Guo model and trace the main progenitors of the central galaxies back in time to analyse whether they have been a satellite in the past.

The top row of Fig. 6 shows the 1 Mpc density dependence of the quiescent fraction of all model centrals (solid lines with yellow shaded areas as shown before in Fig. 3). We additionally distinguish between quiescent centrals having *always* been centrals, i.e. *'true'* centrals, (dashed lines with dark red shaded areas) and quiescent centrals having been *satellites in the past*, i.e. *'backsplash'* centrals (dotted lines and orange shaded areas). For the true and backsplash centrals, we have calculated their quiescent fractions with respect to the *total amount of centrals*, i.e.

$$f_{\rm quiescent} = \frac{n_{\rm qu,bsp/true}}{n_{\rm cent}}, \tag{5}$$

where $n_{\rm qu,bsp/true}$ is the amount of quiescent backsplash or true centrals and $n_{\rm cent}$ the total number of centrals.

This fraction is a superposition of the quiescent fraction with respect to the amount of only backsplash/true centrals ($=n_{\rm qu,bsp/true}/n_{\rm bsp/true}$) and the fraction of backsplash/true centrals ($=n_{\rm bsp/true}/n_{\rm cent}$):

$$f_{\rm quiescent} = \frac{n_{\rm qu,bsp/true}}{n_{\rm cent}} = \frac{n_{\rm qu,bsp/true}}{n_{\rm bsp/true}} \times \frac{n_{\rm bsp/true}}{n_{\rm cent}}, \tag{6}$$

where $n_{\rm bsp/true}$ is the total amount of true/backsplash central galaxies.

The top row of Fig. 6 shows that the quiescent fraction of true central galaxies is not or even negatively correlated with the 1 Mpc density, while the one of the backsplash population is strongly dependent on density. The bottom row of Fig. 6 shows the fraction of backsplash and true centrals ($=n_{\rm bsp/true}/n_{\rm cent}$) versus the 1 Mpc density in different stellar mass bins. It is clear from the figure that the density dependence of the quiescent fraction of backsplash centrals is mainly caused by a strong positive density dependence of the fraction of backsplash centrals.

In the bottom row of Fig. 6, we also give the fractions of backsplash galaxies (with respect to the total number of central galaxies) in each stellar mass bin. About 15 per cent of the lowest mass centrals have been satellites in the past. At fixed stellar mass, the fraction of backsplash centrals increases with increasing density so that e.g. for low-mass centrals residing at densities $\log(\Sigma_{\rm 1Mpc} + 1) > 0.3$ at least 30 per cent of centrals have been satellites in the past. For larger stellar masses, the fraction of backsplash galaxies decreases to about 9 per cent. For galaxies with stellar mass $\log(M_{\rm halo}/{\rm M}_\odot) > 11$, the

Downloaded from https://academic.oup.com/mnras/article/444/3/2938/1062092 by CNRS - ISTO user on 25 April 2022

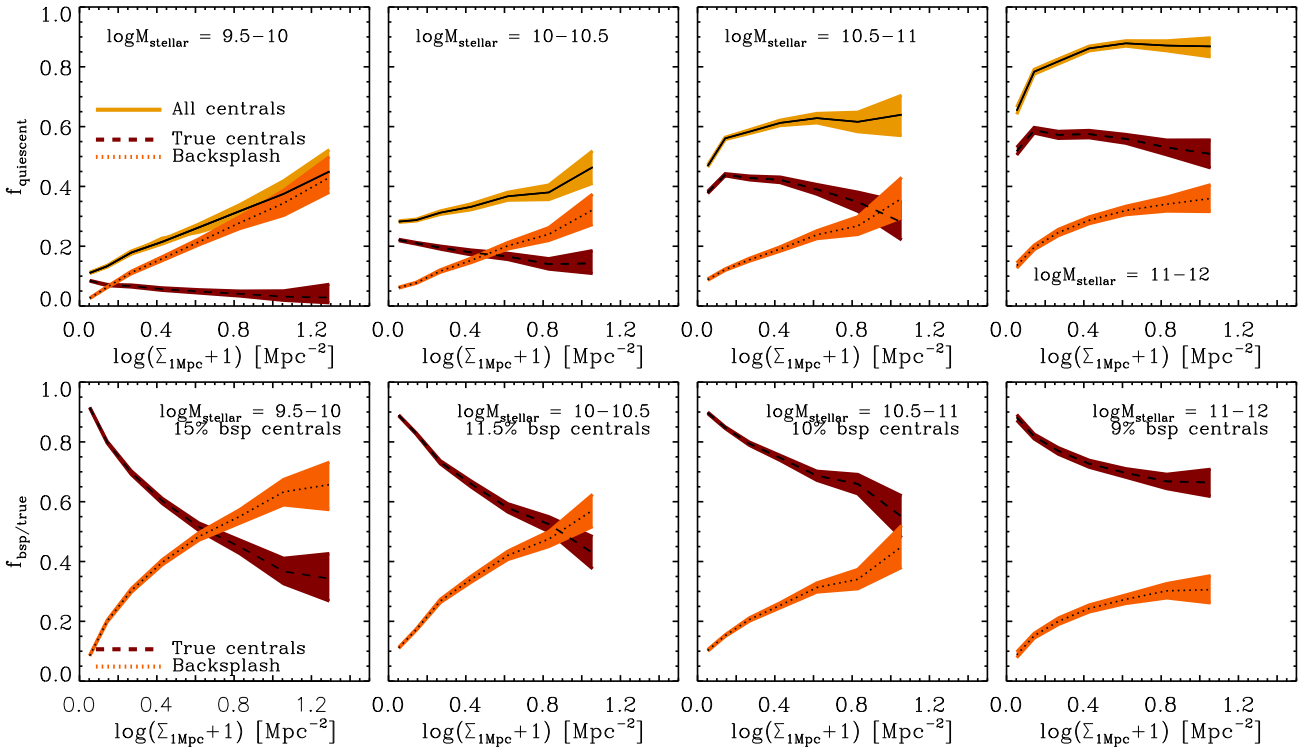


Figure 6. Top row: the quiescent fraction of model central galaxies (solid lines with yellow areas) in different stellar mass bins (different columns) versus the 1 Mpc density distinguishing between centrals having always been centrals (true centrals, dashed lines with dark red areas) and centrals having been satellites in the past (backsplash population, dotted lines with orange shaded areas). The quiescent fractions of backsplash centrals are responsible for the overall density dependence of quiescent model centrals. Bottom row: the total fractions of backsplash (orange) and true (dark red) central galaxies versus the 1 Mpc density in different stellar mass bins. The lower the galaxy stellar mass and the higher the density, the higher is the probability that a central galaxy was a satellite galaxy in the past.

majority of the central galaxies have been centrals for their entire life (almost independently of density).

Our fractions of backsplash centrals are somewhat larger than those found in a recent study by Wetzel et al. (2014): their fractions of ejected/backsplash galaxies is below 10 per cent while we find fractions up to about 15 per cent. We believe that these differences can be ascribed to differences in the algorithm used to identify dark matter haloes and to construct their merger trees (and probably also in the definition for satellite galaxies in the Guo model). Although quantitatively different, however, the trends found for our model galaxies are qualitatively consistent with those found by Wetzel et al. (2014).

In Fig. 7, we analyse the density and stellar mass dependence of some properties of backsplash central galaxies in the models: the top panel shows the median total time $t_{\rm total}$ which backsplash centrals have spent as satellites, the middle panel illustrates the weighted median or effective redshift $z_{\rm weighted}$ at which backsplash centrals have been satellites in the past and the bottom panel shows the weighted median or effective parent halo mass in which backsplash centrals have been residing as satellites – always distinguishing between different stellar mass bins (different line styles). The grey shaded areas illustrate the 25 and 75 percentiles of the different quantities for the lowest stellar mass bin. The dispersion is similar for the higher stellar mass bins.

The weighted or effective redshift for a backsplash central galaxy is estimated as

$$z_{\rm weighted} = \frac{\sum_i (\bar{z}_i \times \Delta t_i)}{t_{\rm total}}, \qquad (7)$$

where $t_{\rm total}$ is the total amount of time the galaxy has spent as a satellite, Δt_i is the time interval during which the galaxy has continuously been a satellite (without any interruption of being a central) and $\bar{z}_i$ is the corresponding average redshift. The weighted halo masses for a backsplash central have been calculated in the same manner (replacing z_i with $M_{{\rm halo},i}$). Such weighted quantities are supposed to give an estimate for the 'typical' redshift, at which backsplash centrals have most likely been satellites, or the mass of a 'typical' parent halo, in which backsplash centrals have been residing in the past.

The top panel of Fig. 7 shows that, on average, backsplash centrals have been satellites for 1–3 Gyr depending on their stellar mass and environment. Generally, the higher the present-day density is, higher is the average total time backsplash centrals have spent as satellites. This is a consequence of hierarchical clustering: present-day high-density regions have most likely emerged out of overdense regions in the past and higher densities give a higher probability of being temporarily accreted on to a massive halo.

For a given density below $\log(\Sigma_{\rm 1Mpc}+1) < 1$ [Mpc^{-2}], low-mass backsplash centrals have been satellites for a somewhat longer time than more massive centrals. This may be a consequence of the orbits: low-mass backsplash galaxies on a pure radial orbit move to a larger apocentre (and thus to a region of lower density) than higher mass ones because dynamical friction is weaker for them. Any high-mass backsplash galaxies which make it out to these regions of low density despite the strong effects of dynamical friction are either escaping a low-mass host halo, or/and just passing by with a relatively large impact parameter. At high density none of this applies, and therefore, more massive backsplash centrals/satellites

Downloaded from https://academic.oup.com/mnras/article/444/3/2938/1062092 by CNRS - ISTO user on 25 April 2022

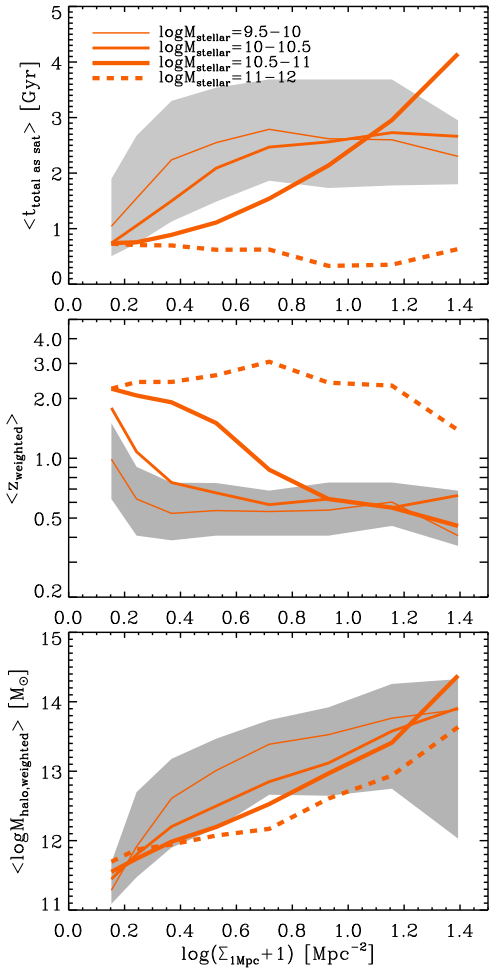


Figure 7. Top panel: average total time backsplash centrals have spent as a satellite versus the present-day 1 Mpc density for different stellar mass bins (indicated by different line styles). Middle panel: median weighted redshift, at which backsplash centrals have been satellites in the past, versus the present-day density for different stellar mass bins. Bottom panel: median weighted parent halo mass, in which backsplash centrals have been residing as satellites, versus present-day density for different stellar mass bins. The grey shaded areas always illustrate the 25 and 75 percentiles of the different quantities for the lowest stellar mass bin.

are likely to have been in more massive haloes for a longer time.

The middle panel of Fig. 7 shows that backsplash centrals have preferentially been satellites at redshifts between $z_{\rm weighted} \sim 0.5-2$. Backsplash centrals of similar stellar mass in high-density regions have been satellites at later times than those in low-density regions. Backsplash centrals in high-density regions have been on average satellites only 5 Gyr ago ($z \sim 0.5$), while those at low-density regions have been satellites 9 Gyr ago ($z \sim 2$).

At a given density below $\log(\Sigma_{\rm 1Mpc} + 1) < 1\,[{\rm Mpc}^{-2}]$, more massive backsplash centrals have on average been satellites at higher redshifts, i.e. a longer time ago, while less massive ones have preferentially been satellites at later times. As a consequence of hierarchical clustering (more massive haloes form later than low-mass ones), low-mass backsplash centrals have been residing in more massive parent haloes than those with high stellar masses and/or those residing at low densities (see the bottom panel of Fig. 7).

To summarize, these results indicate that environmental effects on central galaxies due to the 'backsplash' effect are particularly important for low-mass centrals and for centrals at high densities, as they have typically been satellites more recently. Instead, present-day massive backsplash centrals at low densities may have likely been less affected by environmental processes because they have been satellites in low-mass haloes, when the Universe had only one third of its current age. Since then, they have been evolving like a 'normal' central galaxy.

4.3.2 The spatial extent of environmental effects on superhalo scales

In the previous section, we have demonstrated that for model galaxies the increasing fraction of quiescent centrals as a function of density is partially driven by an increasing fraction of the backsplash galaxies. Observations, however, reveal a somewhat stronger density dependence of quiescent centrals than the models (see Fig. 3). This likely indicates the need for a strengthened influence of environment on central galaxies or a refined treatment of internal processes.

Unfortunately, observations do not allow the significance of a backsplash population and their contribution to the overall environmental dependence of centrals to be probed directly. Observations can, however, be used to estimate out to which scales environmental effects work on centrals and they can help us to assess the scales on which environment is influencing central galaxies most efficiently.

For such an analysis, we follow the multiscale approach presented in a paper by Wilman et al. (2010). They calculate the density of two formally independent, non-overlapping annuli: the one of a smaller scale cylinder and the one of a larger scale annulus. This allows us to extract and to analyse residual effects of the large-scale density on quiescent galaxies on top of the small-scale density. The annulus density is computed as

$$\Sigma_{ri-ra{\rm Mpc}} = \frac{N(ra) - N(ri)}{\pi(ra^2 - ri^2)}, \qquad (8)$$

where $N(ra)$ is the amount of neighbours within a cylinder of radius ra and $N(ri)$ the one within a cylinder of radius ri.

Fig. 8 shows the quiescent central fraction as a function of the smaller scale cylindrical density binned in larger scale and non-overlapping annulus densities (different colours). We have considered three different cylinder-annulus pairs of 0–0.2 and 0.2–1 Mpc (top panel), 0–1 and 1–2 Mpc (middle panel) and 0–2 and 2–3 Mpc (bottom panel). This is shown only for $\log(M_{\rm stellar}/{\rm M}_\odot) = 10-10.5$ galaxies, but the qualitative trends do not change when varying the stellar mass bin. Observations clearly indicate a strong residual effect of the 0.2–1 Mpc scales on top of the 0.2 Mpc density (top panel): the higher the (larger scale) annulus density at a given (smaller scale) cylindrical density is, the higher is the quiescent fraction. Observations do not reveal any significant residual trend for scales beyond 1 Mpc. This is in agreement with previous observational results of Wilman et al. (2010).

As central galaxies with masses $\log(M_{\rm stellar}/{\rm M}_\odot) = 10$–$11$ typically have halo masses of $\log(M_{\rm halo}/{\rm M}_\odot) = 11.5-12.5$ with virial radii of ∼100–200 kpc, the observed environmental trends out to 1 Mpc would imply that effects on superhalo scales should be relevant out to $5-10 \times r_{\rm vir}$. This is in agreement with the study of Wetzel et al. (2014) who find using SDSS data an increased quiescent central fraction out to two times the virial radius of the host halo (see their fig. 1): a massive cluster ($\log(M_{\rm halo}/{\rm M}_\odot) = 14$) has

Downloaded from https://academic.oup.com/mnras/article/444/3/2938/1062092 by CNRS - ISTO user on 25 April 2022

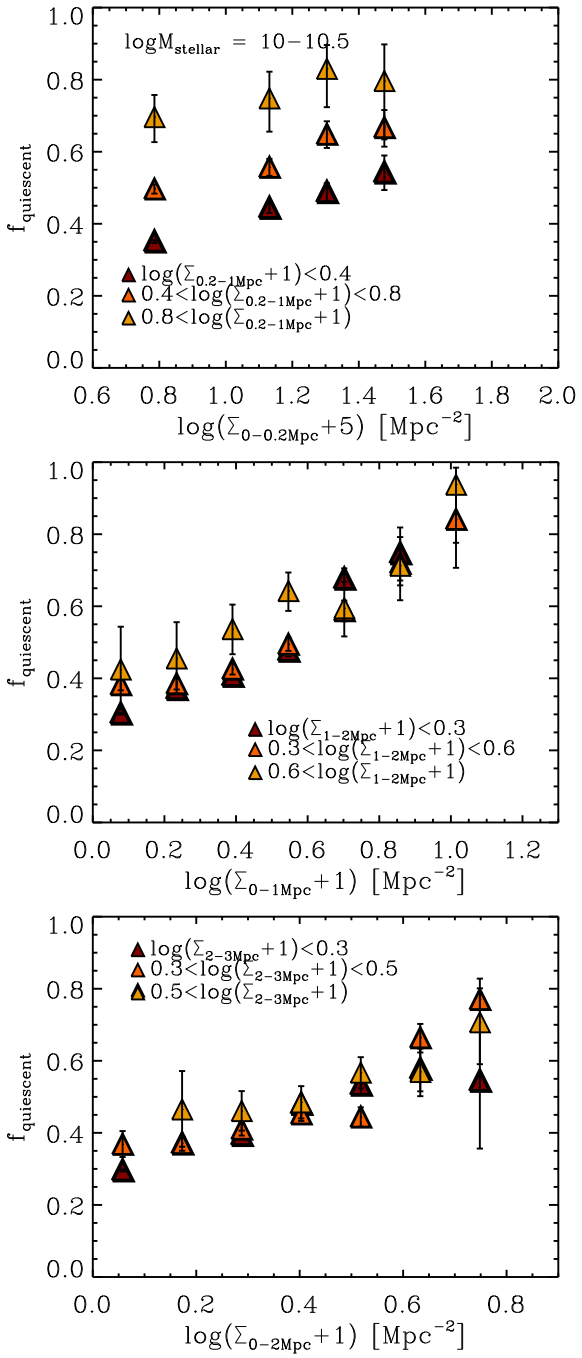


Figure 8. The quiescent fractions of observed central galaxies with masses of $\log M_{\rm gal} = 10$–10.5 versus the smaller scale 0–0.2 Mpc (upper panel), 0–1 Mpc (middle panel) and 0–2 Mpc density (lower panel) binned in different larger scale, non-overlapping annulus densities (0.2–1, 1–2 and 2–3 Mpc, respectively, indicated by different colours and increasing line thickness with decreasing density). Observations mainly reveal a residual effect on the quiescent centrals on scales between 0.2 and 1 Mpc but hardly beyond 1 Mpc.

typically a virial radius of ∼500 kpc so that the quiescent fraction is increased out to a distance of 1 Mpc (from the cluster centre).

In the top row of Fig. 9, we compare models (lines and shaded areas) and observations (symbols, increasing line thickness with decreasing density) for the quiescent fraction of centrals versus the small-scale 0.2 Mpc density, binned in different large-scale 0.2–1 Mpc annulus densities (different colours) and different bins of stellar mass (different panels). While observations show the typical, strong residual effects for *all* stellar mass bins on top of the 0.2 Mpc density, models reveal a clear dependence only at low stellar masses. This trend in the model predictions is similar to the observed one at low densities, but less pronounced than in the observations at high densities. For more massive galaxies ($\log(M_{\rm stellar}/{\rm M}_\odot) > 10$) models do not predict any residual trend – in contrast with observations.

In the middle and bottom row of Fig. 9, we again split the central galaxy sample into backsplash and *true* centrals, respectively, to investigate their contribution to the overall residual effects shown in the top row. As before, the backsplash and *true* central quiescent fraction are estimated with respect to the total amount of central galaxies (see equation 5). This clearly shows that any residual density effect on scales above 0.2 Mpc in the model is caused by the backsplash population.

Low-mass, *true* central model galaxies do not reveal any residual effect of the large-scale density on top of a given small-scale density. For more massive *true* centrals, an anticorrelation between their quiescent fraction and the large-scale density emerges: at a given small-scale density, the fraction of quiescent and *true* centrals increases with decreasing large-scale density. This behaviour can be understood as follows: the fraction of quiescent and *true* centrals (given by equation 6) is the product of the fraction of *true* centrals which are quiescent and the fraction of all centrals which are *true*. The former is not dependent on the (large-scale) density, while the latter (the *true* fraction of centrals) increases with decreasing large-scale density (see bottom row in Fig. 6). This means that the more isolated central galaxies are (lower density), the higher is the *true* fraction of centrals and thus, the probability that they have always been central galaxies. As a consequence, the plotted fraction $n_{\rm qu,true}/n_{\rm cent}$ will increase with decreasing large-scale density (simply because the *true* central fraction is increasing).

The discrepancy between observations and models with respect to the density dependence of quiescent centrals on superhalo scales between 0.2 and 1 Mpc indicates that models might miss environmental effects working on centrals. Possible solutions will be discussed in Section 6.2.2.

4.4 Satellite galaxies

In this section, we turn to quiescent satellite galaxies and explore the physical origin of the density dependence of the quiescent fraction of satellites. We have already pointed out in Section 4.2 that their density dependence is partly caused by the parent halo masses which strongly correlate with the 1 Mpc density in both observations and models. We now examine the role of the projected radial distance of satellites to their parent halo centre.

4.4.1 The relation between density and the projected radial distance to the parent halo centre

Fig. 10 shows that the 1 Mpc density above $\log(\Sigma_{\rm 1Mpc} + 1) > 0.5$ strongly correlates with the radial distance of the satellites to the centre of their parent haloes (normalized to the virial radius of the parent haloes) in both observations (symbols) and models (solid lines with green shaded areas): as expected, satellites closer to the centre of their parent halo are generally residing in denser environments. The relation becomes slightly weaker for higher stellar masses (shown by the different panels). Observations reveal a slightly steeper relation at galaxy masses below $\log(M_{\rm stellar}/{\rm M}_\odot) < 11$. Such a correlation between density and radial distance to the halo centre is also

Downloaded from https://academic.oup.com/mnras/article/444/3/2938/1062092 by CNRS - ISTO user on 25 April 2022

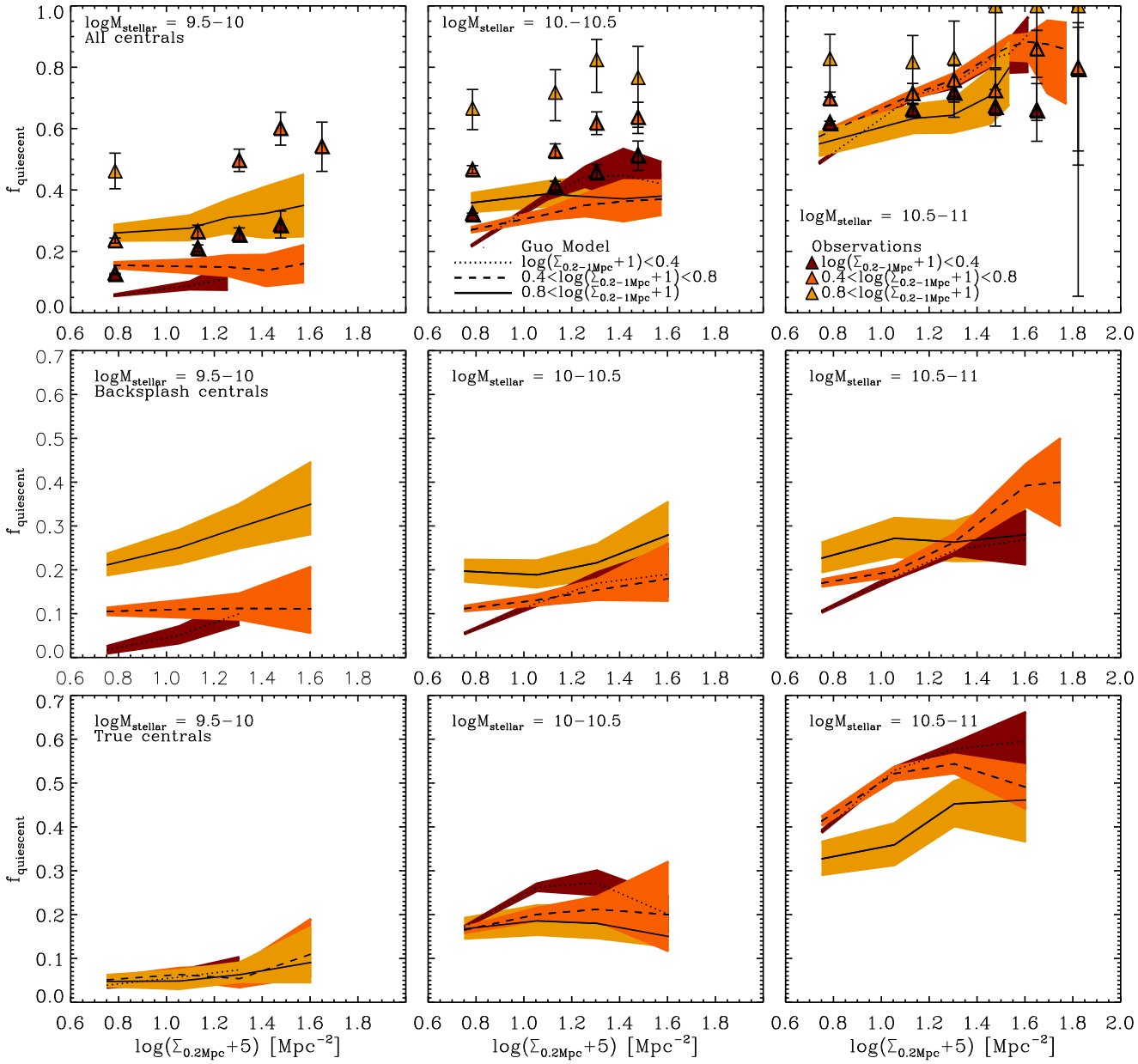


Figure 9. Top row: quiescent fractions of central galaxies are plotted versus the small-scale 0–0.2 Mpc density for different large-scale 0.2–1 Mpc density bins (different colours) in observations (symbols, increasing line thickness with decreasing density) and models (lines with shaded areas). Middle and bottom rows: same as the top row, but now dividing the quiescent central galaxies into backsplash and true centrals, respectively. The quiescent fractions are calculated with respect to the total amount of central galaxies. In the models, any residual effect of density on superhalo scales is caused by the backsplash population of central galaxies.

in agreement with the study of Woo et al. (2013, see their fig. 6) although they use a different density estimator.

For low-density satellites ($\log(\Sigma_{1\mathrm{Mpc}} + 1) < 0.5$, i.e. less than three neighbours within a 1 Mpc cylinder), the radial distance is decreasing with decreasing density. This behaviour is driven by the regime of isolated compact groups, triplets and pairs: the smaller the number of group members is, the smaller and the more compact the groups are, reducing the relative radial distance to the halo centre.

These results imply that the density dependence of quiescent satellites is not only driven by the parent halo mass alone, but also by a trend with radial distance. It should be noted that there is also a correlation between radial distance and accretion time: satellites closer to the centre were accreted on average earlier than those residing at larger distances from the halo centre. Therefore, satellites closer to the centre have been subject to the environment of the halo for longer time.

4.4.2 The dependence of the quiescent satellite fraction on the radial distance

Fig. 11 shows the quiescent satellite fraction versus halo mass in different radial distance bins (as indicated in the legend) for different stellar mass bins (different panels). Observations reveal a strong residual dependence on the radial distance for low-mass satellites ($\log(M_{\mathrm{stellar}}/\mathrm{M}_{\odot}) < 10.5$) in parent haloes with masses

Downloaded from https://academic.oup.com/mnras/article/444/3/2938/1062092 by CNRS - ISTO user on 25 April 2022

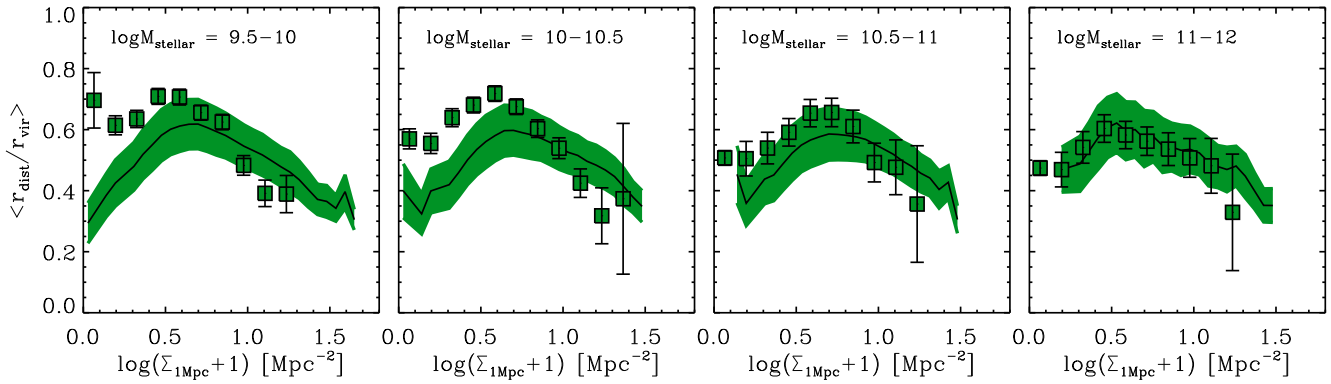


Figure 10. Mean radial distance versus the 1 Mpc density for satellites in different stellar mass bins (different panels) in observations (symbols) and models (lines with shaded areas). Density and radial distance are strongly correlated for densities above $\log(\Sigma_{1\mathrm{Mpc}} + 1) > 0.5$.

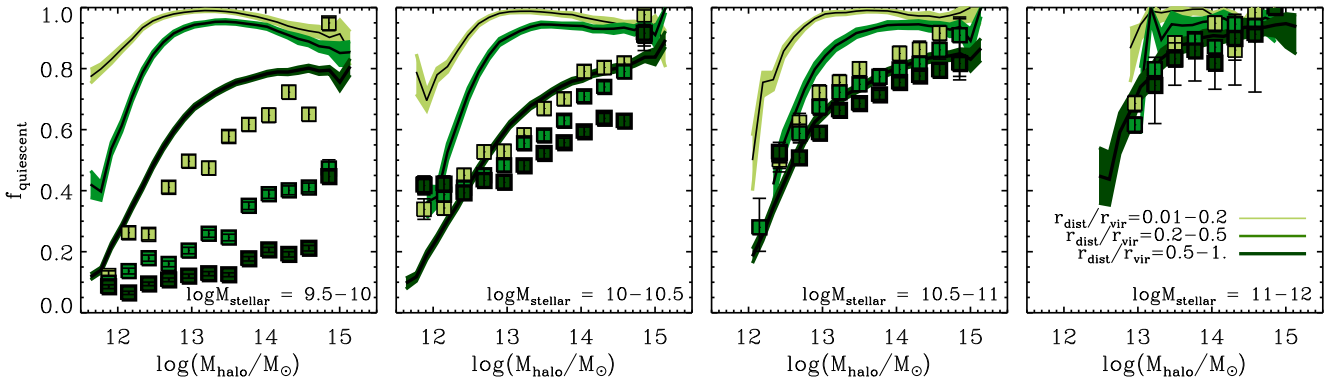


Figure 11. Quiescent fractions of satellite galaxies divided into bins of their radial distance to the halo centre (different colours and line thickness as indicated in the legend) are plotted versus the parent halo mass for observations (symbols, increasing line thickness with increasing distance to the halo centre) and the Guo model (lines with shaded areas). Different panels correspond to different stellar mass bins. Interestingly, observations mainly reveal a dependence on the radial distance for lower mass satellites.

above $\log(M_{\mathrm{halo}}/\mathrm{M}_\odot) > 13$. This is consistent with the observational results presented in Woo et al. (2013).

This may suggest that environmental processes like strangulation, ram-pressure stripping, etc., are most efficiently working on lower mass satellites, but seem to be of less relevance for more massive satellites. The latter may instead be more strongly influenced by internal quenching processes (as stellar or AGN feedback). This agrees roughly with results by Peng et al. (2012) who show that quiescent fractions of low-mass galaxies are mainly dependent on density (and not on stellar mass) indicating the relevance of environment for star formation quenching in this regime.

We have verified (not shown here) that at fixed density and stellar mass, there is hardly any residual dependence on parent halo mass or on radial distance. This means that the increasing fraction of quenched satellites as a function of density is fully explained by the trend as a function of the parent halo mass and radial distance. Equivalently, the halo mass and radial trends can be viewed as components of the trend with density.

In contrast to the observations, model satellites show a significant residual dependence on the radial distance on top of the host halo mass up to large stellar masses of $\log(M_{\mathrm{stellar}}/\mathrm{M}_\odot) = 11$. In addition, models extremely overestimate the quiescent satellite fractions at a given halo mass and radial distance, particularly in the innermost parts of their parent haloes. Low-mass model satellites in low-mass host haloes have a strong dependence on the radial distance, while most of the satellites residing in massive host haloes are already quenched irrespectively of the radial distance. In contrast, observations reveal just the opposite trends.

Overall, these results confirm and strengthen our earlier conclusion that model satellites, particularly the low-mass ones, suffer from too strong environmental effects leading to too short quenching time-scales. Moreover, these strong environmental effects predict excessive residual dependence on the radial distance for $\log(M_{\mathrm{stellar}}/\mathrm{M}_\odot) > 10$ which is not displayed by observations.

5 CONSTRAINING QUENCHING TIME-SCALES FOR SATELLITES

In this section, we estimate which time-scales for quenching star formation in satellite galaxies *should* be predicted by the models so that their quiescent fractions would be consistent with observations. For that, we take advantage of our knowledge of the environmental history of model galaxies and correlate it with observational estimates for the total fraction of satellites that became quiescent after being accreted. These fractions will be referred to as 'transition fractions' and are defined in Section 5.2 below.

To constrain quenching time-scales we make the simple assumption that galaxies are quenched after having spent a given amount of time in a halo more massive than some critical threshold. Comparing the theoretical estimates with the observed transition fractions allows us to constrain both the typical time-scale for quenching and the typical environment (halo mass) where satellite galaxies get quenched.

The fraction of satellites that became quiescent *only after* the infall into their host halo is *not* a directly observable quantity. Indeed, the observed quiescent satellite fraction results from a

Downloaded from https://academic.oup.com/mnras/article/444/3/2938/1062092 by CNRS - ISTO user on 25 April 2022

superposition of environmental and internal quenching processes (some of the quiescent satellites have already been quenched whilst they are still centrals due to internal processes like e.g. supernovae or AGN feedback). Unfortunately, estimating the transition fractions from observations is not straightforward and, as we will discuss below, requires a number of assumptions. Below, we will discuss in detail the caveats in previously adopted definitions of the transition fractions, and will attempt to improve these estimates. Albeit improved, our method is still approximate. For example, one should account for the fact that also *after* infall of a star-forming galaxy, internal processes could be responsible for (or contribute significantly to) quenching its star formation. We will discuss the limitations of our approach in the following.

5.1 Quantifying the environmental history – environmental fractions

To quantify the environmental history of model satellites, we have defined their 'environmental fractions' as the fractions of satellite galaxies (at a given present-day stellar mass and density) which have been residing as a satellite in a halo more massive than X for a time longer than Y. For X and Y, we consider the values $\log(M_{\rm halo}/{\rm M}_{\odot}) = 12$, 12.7, 13 and 3, 5, 7 Gyr, respectively.

Fig. 12 illustrates such environmental fractions (green lines) versus their present-day 1 Mpc density for different stellar mass bins (top row: $\log M_{\rm stellar} = 9.5-10$; middle row: $\log M_{\rm stellar} = 10$–$10.5$; bottom row: $\log M_{\rm stellar} = 10.5-11$). Different columns

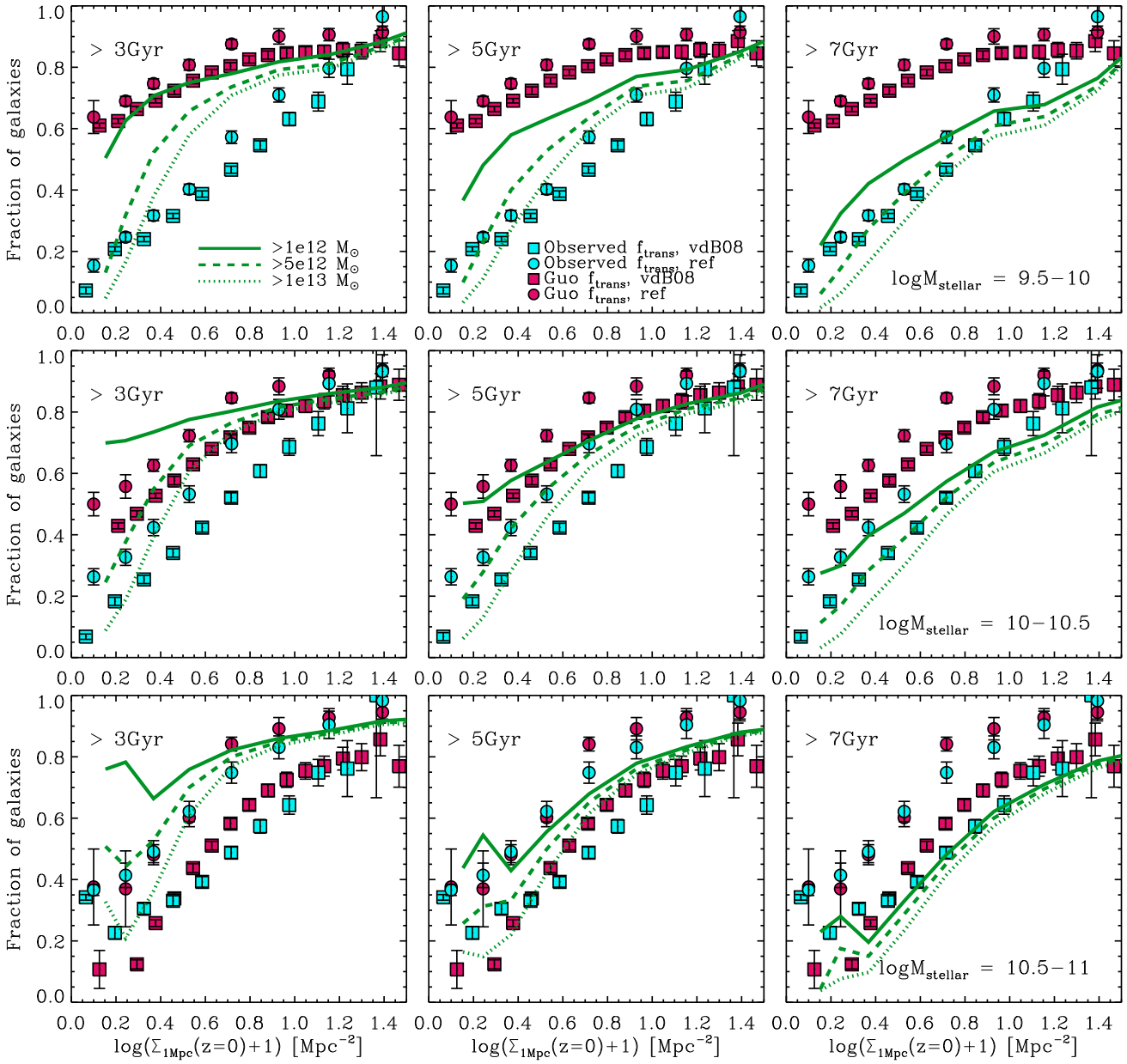


Figure 12. Fraction of model satellite galaxies having spent as a satellite more time than Y in haloes more massive than X (different line styles in green colour) versus the present-day 1 Mpc density for different stellar mass bins (different rows). Different columns correspond to different values of time Y. The squares illustrate the 'vdB' transition fractions, the circles the refined ones. Magenta symbols correspond to the transition fractions derived from the Guo model, while the cyan ones illustrate them derived from the observational data. Comparing the observed refined transition fractions with modelled environmental fractions suggests for low-mass satellites long quenching time-scales of ∼5 Gyr which are decreasing with increasing stellar mass.

Downloaded from https://academic.oup.com/mnras/article/444/3/2938/1062092 by CNRS - ISTO user on 25 April 2022

Table 1. Summary of the quenching time-scales (in Gyr) estimated by the different methods (first and second column: vdB and refined transition fractions based on observations; third and fourth column: vdB and refined transition fractions based on the Guo model; fifth column: directly derived quenching time-scales from the Guo model) for a given stellar mass bin (in $\log M_{\rm stellar}$).

Stellar mass bin	Observed ftrans vdB08	Observed ftrans ref	Guo ftrans vdB08	Guo ftrans ref	Directly calculated from Guo model
9.5–10.0	6	5–6	< 3	< 3	2.5
10.0–10.5	6	3–5	3–4	3	2.9
10.5–11.0	7	3	5	3	2.9

indicate different time limits Y, while different line styles correspond to different halo mass limits X, as indicated in the legend.

At fixed stellar mass and time (Y), the model environmental fractions increase with increasing present-day density for each value of halo mass X. At high density, the difference between lines corresponding to different values of X becomes small: a very high fraction of galaxies in this density range has spent significant amount of their lifetime in massive haloes. At fixed stellar mass, density and time (Y), model fractions decrease with increasing X. This is expected as satellites selected using a higher halo mass limit are just a sub-sample of those corresponding to a lower mass limit. For larger values of Y, model fractions always decrease for fixed density, stellar mass and value of X.

At fixed X and Y, the environmental fractions increase with increasing stellar mass at low densities. For example, more than 70 per cent of galaxies with masses $\log(M_{\rm stellar}/{\rm M}_\odot) = 10$–$10.5$ have been residing as a satellite in haloes more massive than $\log(M_{\rm halo}/{\rm M}_\odot) > 12$ for more than 3 Gyr (solid line in the middle-left panel). For galaxies with masses $\log(M_{\rm stellar}/{\rm M}_\odot) = 9.5-10$, this fraction decreases to 50 per cent at low densities (solid line in the top-left panel of Fig. 12). Otherwise, we hardly find any dependence of the environmental fractions on stellar mass.

5.2 Quenching time-scales derived from transition fractions a la 'vdB'

To obtain an *observational* estimate for the fraction of galaxies that have been quenched only after they became satellites, we begin by using the same approach as adopted by van den Bosch et al. (2008). In particular, we compute their 'transition fractions' as follows:

$$f_{\rm trans} = \frac{(f_{\rm sat,qu}(z_0, M_{z0}) - f_{\rm cent,qu}(z_{\rm inf}, M_{\rm inf}))}{f_{\rm cent,sf}(z_{\rm inf}, M_{\rm inf})}, \quad (9)$$

where $f_{\rm cent,qu/sf}(z_{\rm inf}, M_{\rm inf})$ is the quiescent (resp. star-forming) central fraction at the time of infall and for a given stellar mass at infall and $f_{\rm sat,qu}(z_0, M_{z0})$ is the quiescent satellite fraction at present time. The fractions are calculated with respect to the total number of satellite/central galaxies according to equation (4). The numerator of equation (9) determines the fraction of all satellite galaxies that have undergone a star forming to quiescent transition after their accretion. This decreases with increasing stellar mass simply reflecting that at the massive end, most central galaxies lie already on the 'quiescent sequence'. The denominator determines the fraction of infalling galaxies which were star forming at the time of accretion (which also depends upon mass) – and thus equation (9) gives us the total fraction of galaxies which have become quiescent since accretion. Hence, the transition fractions give an approximate estimate of the fraction of satellite galaxies that have been quenched by environmental processes.

In the study of van den Bosch et al. (2008), they make the simplified assumption that the quiescent central fraction at the time of infall is the same as at the present day:

$$f_{\rm cent,qu}(z_{\rm inf}, M_{\rm inf}) = f_{\rm cent,qu}(z_0, M_0). \quad (10)$$

A further caveat in their study is that they assume no strong evolution of the stellar mass after infall (within the limits of the stellar mass bin considered). These approximations for estimating transition fractions have been used in several recent studies (e.g. De Lucia et al. 2012; Peng et al. 2012; Kovač 2014). In our study (as we need the transition fractions as function of density), we additionally assume that central galaxies have been residing in the lowest density regions when they were accreted, i.e. we take the central fractions at a 1 Mpc density of $\log(\Sigma_{\rm 1Mpc} + 1) \sim 0.1$.

Comparing now the observed transition fractions with the environmental fractions defined in Section 5.1, allows us to constrain the values of X and Y, i.e. the typical environment where satellite galaxies are quenched, and the characteristic time-scale of this process.

The 'vdB' transition fractions extracted from observations are illustrated by the cyan squares in Fig. 12. They best match the model environmental fractions (green lines) where galaxies have been satellites for more than 5−7 Gyr, almost irrespective of stellar mass and the parent halo mass in which they have been living in the past (see the first column in Table 1).

Galaxies in our stellar mass range which have been satellites for >7 Gyr almost all live in haloes with $\log(M_{\rm halo}/{\rm M}_\odot) > 13$ (see the similarity of green lines in the right-hand panel of Fig. 12). This implies that the quiescent fraction is almost entirely determined by the time spent as a satellite in such haloes. The fraction of satellites in even higher parent halo masses (e.g. $\log(M_{\rm halo}/{\rm M}_\odot) > 14$) declines because of the paucity of such haloes ∼5−7 Gyr ago.

5.3 Testing the reliability of the vdB transition fractions with models

We now explicitly test the reliability of the approximation used in the previous section by taking advantage of the SAM results: first, we treat predictions from the Guo model like observational data, and estimate typical quenching time-scales by calculating the 'vdB' transition fractions according to equations (9) and (10). Such model 'vdB' transition fractions are illustrated in Fig. 12 by the magenta squares. Their best match with environmental fractions suggests quenching time-scales <3 Gyr for satellites with $\log(M_{\rm stellar}/{\rm M}_\odot) = 9.5-10$, ∼3−4 Gyr for satellites with $\log(M_{\rm stellar}/{\rm M}_\odot) = 10$–$10.5$ and ∼5 Gyr for satellites with $\log(M_{\rm stellar}/{\rm M}_\odot) = 10.5-11$ (see the third column in Table 1).

Secondly, we compute the average quenching time-scales of model satellites by using the full assembly and merger histories of model galaxies. In particular, for each model galaxy, we trace its most massive progenitor back in time and compute the time since when the galaxy was last a star-forming central until it was for the first time a quenched satellite. If the vdB approximation were correct, we would, of course, expect to obtain *the same* quench-

Downloaded from https://academic.oup.com/mnras/article/444/3/2938/1062092 by CNRS - ISTO user on 25 April 2022

ing time-scales by the direct and indirect (vdB) methods. For low-mass satellites the directly derived quenching time-scale is in rough agreement with the one estimated from the 'vdB' transition fractions (2.5 Gyr). For more massive satellites ($\log(M_{\rm stellar}/{\rm M}_\odot) = 10$–$11$), however, models have satellite quenching time-scales of 2.9 Gyr (see the last column in Table 1), significantly shorter than those predicted by the 'vdB' approach based on the Guo data (third column in Table 1).

This discrepancy likely has its origin in the simplified assumptions at the basis of the 'vdB' transition fractions. In particular, the quiescent central fraction at the time of infall may be different to the present-day one. The observational situation is not clear, e.g. Knobel (2013) do not find any redshift evolution of the red central fraction at a given stellar mass, while Tal et al. (2014) find a strong z-dependence for the cumulative red central fractions. To overcome some of the limitations of the 'vdB' transition fractions, we have defined and estimated 'refined' transition fractions $f_{\rm trans,\,ref}$ that we detail in the following section. We note that part of the discrepancy could be also due to the assumed strong correlation between the time spent in a halo and the efficiency of quenching (i.e. to the very same definition of our environmental fractions).

5.4 Quenching time-scales derived from refined transition fractions

For the calculation of the 'refined' transition fractions $f_{\rm trans,ref}$ we also use equation (9), but in contrast to van den Bosch et al. (2008), we now explicitly compute the quiescent (resp. star-forming) central fraction at the time of infall by following the estimation of a recent study of Wetzel et al. (2013):

$$f_{\rm cent,qu}(z_{\rm inf},\,M_{\rm inf}) = \frac{f_{\rm all,qu} - f_{\rm sat,qu}\,f_{\rm sat}}{1 - f_{\rm sat}}. \qquad (11)$$

Here, all quantities are at the time of infall for a given infall stellar mass, $f_{\rm all,qu}$ is the quiescent fraction of all galaxies ($=n_{\rm qu}/n_{\rm all}$) and $f_{\rm sat}$ is the satellite fraction ($=n_{\rm sat}/n_{\rm all}$). As observations do not provide all required information, we combine information on the satellite accretion history and fractions from the models (which are mainly based on dark matter N-body simulations and should be, thus, robust and model independent) with the evolution of the total quiescent fraction in the observations:

(i) first, for a given present-day stellar mass and density, we estimate the average infall times and infall masses of satellites using the galaxy merger trees from the models and following back in time the progenitor galaxies on the main branch;

(ii) secondly, we use observed stellar mass functions of quiescent and star-forming galaxies (Ilbert 2013) to estimate the quiescent fractions of all galaxies $f_{\rm all,qu}$ at the average time of infall for a given average infall stellar mass (calculated from the assembly history of the models) and

(iii) thirdly, we extract the satellite fraction $f_{\rm sat}$ at the time of infall (and a given stellar mass bin at that time) from the models.

In addition, we impose no evolution of the quiescent satellite fraction $f_{\rm sat,qu}$, i.e. we assume that it is the same at the time of infall as in today's Universe:

$$f_{\rm sat,quench}(z > 0) = f_{\rm sat,quench}(z = 0). \qquad (12)$$

This choice is justified by Tinker & Wetzel (2010) who found no evolution in the quiescent fraction for satellites at fixed magnitude at $z \leq 1$ based on halo occupation modelling. We have also explicitly tested the effect of an evolving quiescent satellite fraction with redshift using the results of the observational studies of Mok et al. (2013) and McGee et al. (2011), and find that the results do not change significantly.

The 'refined' transition fractions are illustrated by the cyan circles in Fig. 12. For low-mass satellites $\log(M_{\rm stellar}/{\rm M}_\odot) < 10$, they are in agreement with the 'vdB' transition fractions and suggest quenching times of $\sim$5 Gyr. For more massive satellites, the differences between the 'vdB' and the 'refined' transition fractions become larger, and the latter ones suggest quenching time-scales of 3−5 Gyr for satellites with $\log(M_{\rm stellar}/{\rm M}_\odot) = 10$–$10.5$ and relatively short quenching time-scales of $\sim$3 Gyr for massive satellites with $\log(M_{\rm stellar}/{\rm M}_\odot) = 10.5$−$11$ (see the second column in Table 1). Therefore, the refined fractions suggest quenching time-scales that depend on stellar mass (are longer for low-mass satellites than for massive ones).

To again test the reliability of the refined approach, we compute – as before for the 'vdB' method – the refined transition fractions of the Guo model (see the magenta circles in Fig. 12). They suggest quenching time-scales of $<$3 Gyr for satellites with $\log(M_{\rm stellar}/{\rm M}_\odot) = 9.5$−$10$ and of $\sim$3 Gyr for satellites with $\log(M_{\rm stellar}/{\rm M}_\odot) = 10$–$11$ (see the fourth column in Table 1). These estimates are now consistent with the quenching time-scales directly derived from the Guo model demonstrating *the improvement of this refined method*.

We also point out that for massive satellites with $\log(M_{\rm gal}/{\rm M}_\odot) = 10.5$−$11$ the refined transition fraction from the Guo model and from the observations are in reasonably good agreement which reflects the fact that the models match the observed density dependence of the quiescent satellites in that mass range (see the top row in Fig. 3).

5.5 Caveats

We have demonstrated that the refined approach for constraining quenching time-scales is an improvement compared the 'vdB' method, but there is still one caveat: how the stellar mass of a satellite galaxy evolves after infall (and thus, in which stellar mass bin satellites end at $z = 0$) is strongly model dependent. Satellites can experience stellar stripping (e.g. Pasquali et al. 2010) and therefore, be less massive at $z = 0$, or/and can continue forming stars at a significant rate and therefore, become more massive at present.

The Guo model includes some prescriptions for both processes, but the extent to which their predictions are robust is unclear. To assess the influence of uncertainties of these prescriptions, we consider two extreme scenarios: first, only a decreasing stellar mass due to stellar stripping and secondly, only an increasing stellar mass due to residual star formation. In these scenarios, the same satellite galaxy can end up in a different stellar mass bin at $z = 0$ which may influence the final estimation of the quenching time-scales.

For the first scenario, we compute the average decrease in stellar mass (due to stellar stripping) as a function of the stellar mass at time of infall by using a fitting formula extracted from controlled simulations of galaxy groups (Contini et al. 2014; Villalobos et al., in preparation):

$$M_{\rm strip}(t) = M_{\rm st}(t_{\rm inf})\exp\left[\frac{-16}{1-\eta}\sqrt{\frac{M_{\rm sub}}{M_{\rm par}}}\left(1 - \frac{t}{t_{\rm merg}}\right)\right]. \qquad (13)$$

Here, $M_{\rm st}(t_{\rm inf})$ is the stellar mass at the time of infall, η is the circularity of the orbit, $M_{\rm sub}$ and $M_{\rm par}$ are the subhalo and the parent dark matter halo mass, respectively, and $t_{\rm merg}$ is the residual

Downloaded from https://academic.oup.com/mnras/article/444/3/2938/1062092 by CNRS - ISTO user on 25 April 2022

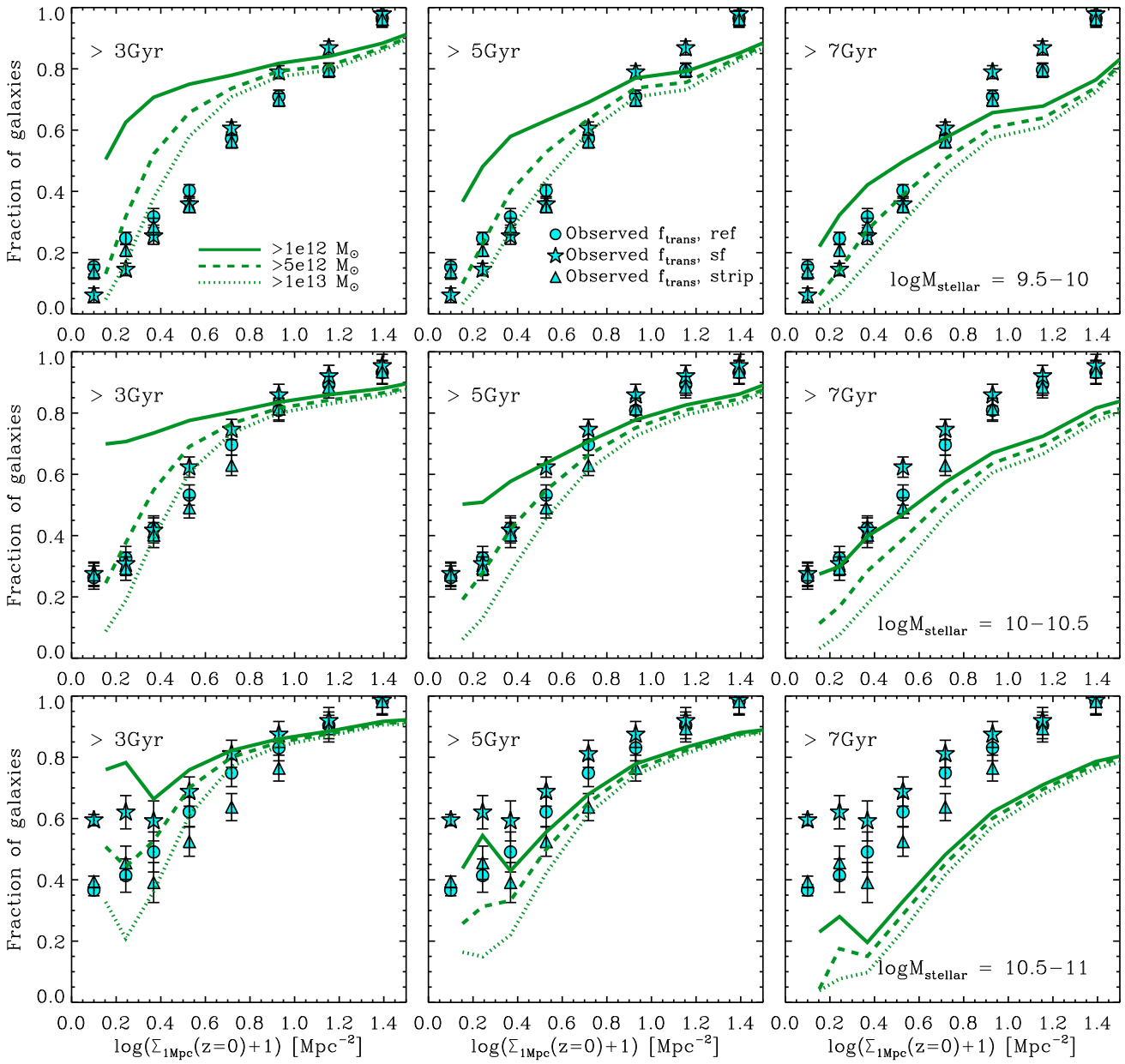


Figure 13. Same as in Fig. 12, but in addition, the cyan stars and triangles illustrate the refined transition fractions derived from observations when two extreme scenarios for the evolution of the stellar mass after infall are assumed: either the satellite stellar mass decreases due to stellar stripping or it increases due to continued star formation. The inaccuracy arising from these processes does not influence the resulting quenching time-scales for satellites.

merger time of the satellite galaxies. Merger times are estimated from a formula (again derived from controlled group simulations) of Villalobos et al. (2013) which is a refinement of the one presented in Boylan-Kolchin, Ma & Quataert (2008). As value for the circularity, we use the one of the most likely infalling orbit ($\eta = 0.51$). The stellar and halo masses are taken directly from the model at the time of infall.

For the second scenario (only increasing stellar mass due to residual star formation), we assign to each infalling galaxy an SFR using the observed relation between the SFR and stellar mass (Daddi et al. 2007; Elbaz et al. 2007) at the time of infall. By assuming that the SFRs stay constant after accretion we compute the average increase in stellar mass for satellite galaxies since they have become a satellite.

Fig. 13 shows the refined transition fractions (cyan circles) and the ones for the purely star forming and the purely stellar stripping scenario (cyan stars and cyan triangles, respectively). For the lowest stellar mass bin (top row), hardly any differences arise between the transition fractions derived from the different scenarios. Towards more massive satellites (middle and bottom row in Fig. 13), however, the differences become larger, particularly for satellites with $\log(M_{\rm stellar}/{\rm M}_{\odot}) = 10.5{-}11$ residing in low-density regions (up to 50 per cent larger transition fractions for the star-forming scenario).

Nevertheless, the uncertainties in deriving the transition fractions based on scenarios of a pure increase or a pure decrease in the stellar mass of an accreted galaxy are not large enough to change the main result: the resulting quenching time-scales when comparing

Downloaded from https://academic.oup.com/mnras/article/444/3/2938/1062092 by CNRS - ISTO user on 25 April 2022

the different transition fractions to the environmental fractions are hardly influenced by the stellar evolution of the satellite after infall.

6 DISCUSSION AND CONCLUSIONS

6.1 Comparison of our observational results to previous studies

Our observational results for the density dependence of quiescent satellite galaxies agree qualitatively with previous observational studies of the present-day Universe (e.g. Peng et al. 2012; Woo et al. 2013; Kovač 2014). These studies also highlight – even if using different density estimators – a strong density dependence of the quiescent satellite fractions at a given stellar mass.

In contrast, for the density dependence of quiescent central galaxies, the situation is less clear: Peng et al. (2012) and Kovač (2014) find no significant density dependence on top of the stellar mass dependence, while the quiescent fractions of low-mass centrals depend, albeit weakly, on density in the study of Woo et al. (2013). These differences may be ascribed to different estimators for quiescence (e.g. colour is used in Peng et al. 2012), to different definitions of environment, to redshift measurement errors, and to the used tracer/neighbour galaxies and their sampling rate (e.g. Kovač 2014 has a significantly lower sampling rate than ours). Therefore, it is generally difficult to directly compare our observational results with previous ones in the literature.

Nevertheless, fig. 1 by Peng et al. (2012) shows that they also *do find* a weak density dependence of central galaxies at high densities (the trend is not as steep as the one for satellites). The statistical significance is, however, low because of the low numbers of central galaxies at high densities. As noted above, Peng et al. (2012) have used optical colours to distinguish between quiescent and star-forming galaxies, which is less accurate than using sSFR (see e.g. Woo et al. 2013). In addition, they might select bluer neighbours (due the *B*-band observations) which are less clustered than redder ones.

In agreement with previous studies, we find that the global density dependence is mainly driven by satellite galaxies, as the vast majority of galaxies residing in denser regions are satellite galaxies, while the majority (∼85 per cent) of central galaxies are located in lower density regions. Even if the central galaxies residing in denser regions show a similarly steep dependence on environment as satellites, they constitute only a minor contribution to the overall galaxy population in these regions (but still non-negligible to the central population). Therefore, one striking result compared to previous studies is the extremely similar behaviour of quiescent centrals and satellites at a given density and stellar mass.

6.2 Model limitations and future perspectives

6.2.1 Satellites

The overproduction of quiescent satellite galaxies in models is a well-known problem (e.g. shown in Kimm et al. 2009 using different SAM) and often attributed to simplified recipes for environmental processes, such as the assumption of an instantaneous strangulation. Our results demonstrate that even the more relaxed, delayed strangulation assumption in the Guo model is not sufficient to solve the 'overquenching problem' of satellite galaxies with masses below $\log(M_{\rm stellar}/{\rm M}_{\odot}) < 10.5$. We have verified that a model assuming an instantaneous stripping of the hot gas and adopting a different definition for satellite galaxies, where environmental processes effectively start when a galaxy enters an FOF group (we have considered the public catalogues based on the De Lucia & Blaizot 2007 model), predicts an even larger fraction of quiescent satellites up to stellar masses of $\log(M_{\rm stellar}/{\rm M}_{\odot}) = 11$. Therefore, the gradual stripping (and different satellite definition) assumed in the Guo model does influence the evolution of satellite galaxies bringing model predictions in better agreement with data. But the effect does not appear to be sufficient to solve the problem of the excess of passive satellites.

There have also been attempts to improve the modelling of environmental processes, e.g. by Font et al. (2008) or Weinmann et al. (2010), but none of them are completely successful in matching the observational data. This shows, that the recipes for environmental effects working on satellite galaxies need to be further refined.

In a recent study, Henriques et al. (2013) have shown that better agreement with data can be obtained assuming a different scaling for the re-accretion time-scale of gas. In their model, low-mass galaxies form later, are typically younger and more star forming than in the Guo et al. model. It will be an important further test for this model to investigate how well it can predict the global environmental dependences of quiescent satellites. It is likely that additional changes for the tidal and ram-pressure stripping will be necessary in order to capture the observed strong dependence on density for low-mass satellites and predict long quenching time-scales of 5 Gyr for low-mass satellites as estimated in this study.

6.2.2 Centrals

We have shown that models cannot predict the similar environmental behaviour of centrals and satellites in the sense that models cannot capture the observed strong density dependence of quiescent central galaxies, particularly the one on superhalo scales (0.2–1 Mpc). Two effects should be considered in this case.

On the one hand, *true centrals* might suffer from environmental effects by directly interacting with an extended hot halo beyond the virial radius. This effect was e.g. investigated by Bahé et al. (2013) using hydrodynamical simulations and was shown to lead to a slow stripping of the hot halo component of the infalling central galaxy. The corresponding effect on the cold gas and star formation is, however, rather weak in the simulations. Such an additional effect might help models to capture a residual environmental effect on 0.2–1 Mpc scales for galaxies more massive than $\log(M_{\rm stellar}/{\rm M}_{\odot}) > 10.5$, where *true* centrals are the dominant contribution to the overall central population.

On the other hand, backsplash centrals may still feel the gravitational potential of their parent halo and may, thus, continue to experience strangulation, i.e. a stripping of their hot gas, even if they have left their parent halo again. Or another, maybe more likely possibility is that backsplash centrals which have passed through the main (host) halo, no longer live inside a filament which would provide them with a continuous supply of gas (as with *true* centrals). Therefore, their star formation continues to exhaust their existing gas content as if they were still satellites.

A recent study of Wetzel et al. (2014), using empirical models for galaxy formation, has shown that such a continued treatment of backsplash centrals as satellites results in good agreement with observational data. In our models, such an assumption could essentially increase the density dependence on superhalo scales for low-mass galaxies and galaxies residing at high densities where the fraction of backsplash centrals dominates. Overall, such processes

Downloaded from https://academic.oup.com/mnras/article/444/3/2938/1062092 by CNRS - ISTO user on 25 April 2022

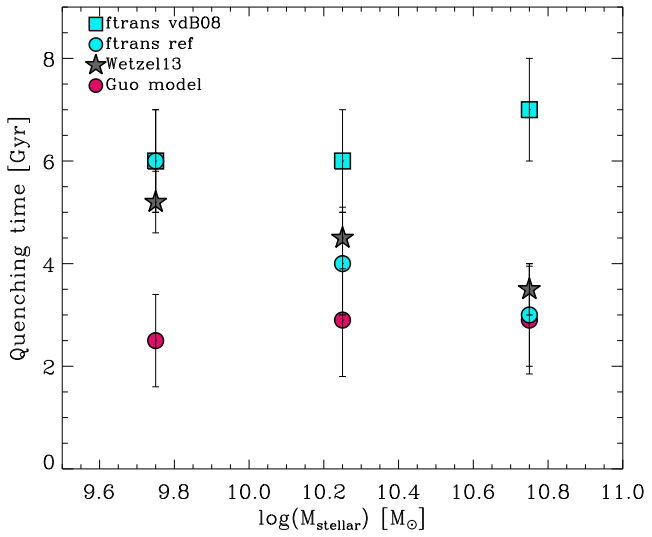


Figure 14. Quenching time-scales estimated from transition fractions ('vdB' method: blue squares, refined method: blue circles) and directly from the Guo model (magenta circles) versus stellar masses. The quenching times scales estimated from the refined transition fractions are in rough agreement with the results from Wetzel et al. (2013, grey stars) and are increasing with decreasing stellar mass.

are not taken into account in the models, but seem to be important to capture the observed environmental trends on superhalo scales.

6.3 Satellite quenching time-scales and their stellar mass dependence

Fig. 14 summarizes the different estimates/predictions for the satellite quenching time-scales from Section 5 summarized in Table 1 showing them as a function of stellar mass. The 'vdB' transition fractions (cyan squares) suggest large quenching time-scales of roughly $\sim$5$-$7 Gyr independent of mass in agreement with a recent study of De Lucia et al. (2012). However, the 'vdB' estimate refers simply to the difference between centrals and satellites at $z = 0$, whereas our refined method estimates the total fraction of satellites *quenched since infall*. The refined transition fractions (cyan circles in Fig. 14) – even when considering the uncertainty due to star formation and stellar stripping of the satellite stellar mass after infall – point towards increasing quenching time-scales with decreasing stellar mass and predict long quenching time-scales of $\sim$5 Gyr for low-mass satellites.

In the Guo model (magenta circles in Fig. 14), the satellites have typically short quenching time-scales, also nearly independent of stellar mass. They agree with our estimates based on the SDSS data for massive satellites, but are significantly underestimated for low-mass satellites ($\sim$2.5 Gyr).

Interestingly, quenching time-scales predicted by the refined approach and their mass dependence are in good agreement with the results of a recent study of Wetzel et al. (2013) using a completely different approach based on an empirical HOD model (see the grey stars in Fig. 14). In their model, they find a 'delayed-then-rapid' quenching scenario to reproduce the observed quiescent satellite fraction and the bimodality of the SFRs. In their proposed scenario, satellite SFRs evolve unaffected for the first several Gyr after infall, after which the star formation quenches rapidly (assuming an exponential decline).

Note that also the results of other studies (Skibba & Sheth 2009; Kang & van den Bosch 2008; Font et al. 2008; van den Bosch et al. 2008) imply that satellite quenching processes must be gradual or delayed and/or that the mechanism (e.g. strangulation) must operate in both group and cluster-mass haloes.

The stellar mass dependence of the quenching time-scales appears counterintuitive at first sight as environmental processes are expected to more easily affect low-mass satellites due to their low internal binding energies. The physical origin of this mass dependence is likely twofold.

First, internal quenching processes such as AGN feedback are working more efficiently on more massive satellites than on less massive ones, reducing their quenching time-scales after infall in addition to the environmental effects they are experiencing. In other words, for more massive satellites, environmental quenching is not the main/only quenching effect. This means that the galaxy status does not matter for massive galaxies to first order. Such an (additional) internally quenched population would also be consistent with the independence of the quiescent fractions for massive satellites on the radial distance as seen in Fig. 11. The difference between the 'vdB' or 'refined' transition fractions is not necessarily enough to separate such additional internal processes *after accretion*. In the (perhaps extreme) case that satellites would experience the same amount of internal quenching as central galaxies (at fixed stellar mass), the'vdB' transition fractions (showing no stellar mass dependence) would represent the fraction of *environmentally quenched* satellites as opposed to the *total* fraction of quenched satellites as expressed by the refined transition fractions. In reality, we may expect the fraction quenched due only to environmental processes to be somewhere between the 'vdB' and the refined transition fractions: satellite galaxies with their own sub-halo probably still experience some (possibly reduced) quenching related to reduced gas accretion and increased heating from massive galaxies (i.e. internal processes), similar to central galaxies.

Secondly, different orbits and dynamical friction time-scales for satellites of different masses may also influence the quenching time-scales. The dynamical friction time-scales are strongly dependent on the ratio between satellite and host halo mass (e.g. Boylan-Kolchin et al. 2008; Villalobos et al. 2013), i.e. the smaller the satellite galaxy (at a given host halo mass), the longer is its dynamical friction time-scale. This implies a longer spiralling around in the outer, low-density regions for low-mass satellites before they get into the denser, inner regions where environmental processes become more efficient. The rate at which gas is removed from a satellite is most likely related to how often it has crossed the higher density medium along its orbit. This means that a satellite could retain more gas if it is exposed less often to the high density of the central regions of the host halo. For the stellar component, this is shown by Villalobos et al. (in preparation) and it is plausible to assume that the gas will behave similarly.

This would also provide a physical explanation for the 'delayed-then-rapid' quenching scenario of the study of Wetzel et al. (2013), where the rapid (exponentially decreasing) quenching may only start when the satellite has reached the dense inner regions of the halo. In contrast, massive satellites have short dynamical friction time-scales and reach the central, dense regions rapidly so that their gas gets stripped efficiently in a short time (even though their internal potential well is deeper). In addition, massive galaxies will more rapidly merge with the central galaxy and then drop out of the satellite population. These will be the ones which have been in the parent halo longest and so have also been most likely quenched,

Downloaded from https://academic.oup.com/mnras/article/444/3/2938/1062092 by CNRS - ISTO user on 25 April 2022

but are lost by merging. This means that massive galaxies cannot have long quenching times because otherwise we would not see any difference between the massive central (infall) and massive satellite quiescent fractions as there would be no time for environmental quenching before they merge away.

The relative contribution of the two scenarios (internal quenching and orbits/dynamical friction time-scales) on the mass dependence of quenching satellites is unclear. We plan to address this issue in a future work.

6.4 Satellite quenching time-scales at higher redshifts

The analysis in this paper only focuses on the present-day Universe. At higher redshifts, however, the Universe is apparently not old enough for such long quenching time-scales as we infer at low redshifts. One explanation for this apparent disagreement is that the currently used models do not properly account for the internal quenching processes. Another, possibly complimentary option is that it is very likely that the quenching time-scale scales vary with the dynamical time, i.e. depend (in addition to halo mass, galaxy mass and density) on redshift and are thus, shorter at higher redshift. The latter possibility is in agreement with results from the work by Mok et al. (2014) who provide constraints for quenching time-scales using observations of groups at $z \sim 0.4$ and $z \sim 0.9$. They find that the observed fractions are best matched with a model that includes a delay (when quenching starts) that is proportional to the dynamical time followed by a rapid quenching time-scale of $\sim$0.25 Gyr.

6.5 Summary

In this study, we have performed a detailed analysis of the effect of environment and the environmental history on quenching star formation in satellite and central galaxies. We have taken advantage of publicly available galaxy formation catalogues where the galaxy formation model of Guo et al. (2011) has been applied to the dark matter Millennium simulation. The Guo model adopts a gradual strangulation of the hot gas content of a satellite galaxy, i.e. the hot halo gas is assumed to be stripped at the same rate as the dark matter halo. We have compared model predictions to observational data of the present-day Universe making use of a refined density catalogue of Wilman et al. (2010) based on the SDSS-DR8 data base and cross-correlated with the catalogues of Brinchmann et al. and Yang et al. To select quiescent galaxies, we have used sSFRs as a tracer, and as an estimator for environment we have considered the theoretical halo mass and projected densities within cylinders with two different radii (0.2 and 1 Mpc). Our main results are as follows.

(1) Observations reveal a surprisingly similar behaviour for the environmental dependence of the quiescent fraction of centrals and satellites. Models cannot capture the observed trends and predict a significantly different behaviour for centrals and for satellites. In particular, they significantly overestimate the quiescent fractions of satellites and slightly underestimate the ones of centrals at fixed stellar mass. In addition, models predict a much weaker dependence on environment for low-mass galaxies than observed.

(2) The dependence of (low-mass) model and observed central galaxies on the 1 Mpc density is not driven by their halo masses, but has its origin in environmental effects on superhalo scales up to 1 Mpc. The density dependence in the models is solely caused by a population of backsplash centrals, which have been satellites in the past and thus, could have experienced environmental effects over time-scales of typically 1.5–3 Gyr. Such backsplash centrals preferentially have low masses and reside in dense environments. However, observations indicate a stronger density dependence of the quiescent centrals on superhalo scales between 0.2 and 1 Mpc. This suggests that models might miss some processes (e.g. a 'satellite-like' treatment of backsplash centrals).

(3) The strong density dependence of (low-mass) satellite galaxies can be understood as the result of a superposition of their host halo mass and their distance to the host halo centre, in agreement with e.g. Woo et al. (2013). At a given radial distance, host halo mass and satellite stellar mass, models significantly overestimate the quiescent satellite fractions compared to observations, indicating that environmental effects are working too efficiently on satellites, particularly the low-mass ones, resulting in too short gas consumption time-scales.

(4) Considering the environmental history of model satellite galaxies and comparing it to transition fractions derived from observational data, we have constrained typical quenching time-scales for satellites. We have improved the estimation of transition fractions compared to a previous study of van den Bosch et al. (2008) by explicitly accounting for a time evolution of the quiescent/star-forming fraction of central galaxies. This allows for more robust and reliable predictions for quenching time scales: we find for low-mass satellites long quenching time-scales of $\sim$5 Gyr. Quenching time-scales are decreasing with increasing stellar mass. For higher mass galaxies, it is less clear, but the quenching time-scales seem to be between 3and5 Gyr depending on the method used.

In this paper, we have pointed out some typical failures of currently used galaxy formation models and with the help of observations we have indicated possible directions towards which models should be improved in future. Our results indicate that models require an improved prescription of environmental processes and internal processes where centrals and satellites should be treated in a much more similar way than done so far: backsplash central galaxies should not experience further filamentary accretion, while satellite galaxies which have retained some of their own halo should still experience AGN/radio-mode/stellar feedback which can lead to internal suppression of star formation. Within the framework of our models, however, it might be difficult to obtain long quenching time-scales *just* as consequence to an improved prescription of environmental processes. Fundamental changes in the models for star formation, stellar feedback and re-accretion are likely required.

In addition, our results highlight the highly important role of orbits and dynamical friction time-scales for the quenching time-scales of satellites and backsplash centrals. They may also help us to resolve the apparent contradiction our results imply for centrals and satellites: while backsplash centrals are supposed to experience stronger environmental effects to get quenched more efficiently, satellites should have much longer quenching time-scales resulting in a much smaller quiescent fraction. Backsplash centrals are sitting on highly eccentric and thus, radial orbits. They can, therefore, rapidly encounter one or more pericentre passages which causes a fast (continuous) stripping of the gas content. Instead, low-mass satellites on tangential orbits and long dynamical friction time-scales reside for a long time in the outer, low-density parts of their host halo without any significant stripping of their gas content and thus, resulting in long quenching time-scales and (relatively) low quiescent fractions.

In future studies, we plan to quantify and to parametrize the evolution of the gas content of centrals and satellites as a function of stellar mass, parent halo mass, their orbits and dynamical friction

Downloaded from https://academic.oup.com/mnras/article/444/3/2938/1062092 by CNRS - ISTO user on 25 April 2022

time-scales using controlled simulations of galaxy groups and clusters. Such parameterisations can be easily implemented in galaxy formation models, and tested against observations.

ACKNOWLEDGEMENTS

MH, GDL and ÁV acknowledge financial support from the European Research Council under the European Community's Seventh Framework Programme (FP7/2007-2013)/ERC grant agreement no. 202781. MH additionally acknowledges support from the European Research Council via an Advanced Grant under grant agreement no. 321323NEOGAL. DW acknowledges support from the Max Planck Gesellschaft (MPG) and the Deutschen Forschungsgemeinschaft (DFG). SW acknowledges funding from ERC grant HIGHZ no. 227749. SZ has been supported by the EU Marie Curie Integration Grant 'SteMaGE' Nr. PCIG12-GA-2012-326466 (Call Identifier: FP7-PEOPLE-2012 CIG). We thank Xiaohu Yang for providing the (unpublished) DR7 version of his group catalogues and the corresponding mock group catalgoue based on the Guo model, and we are grateful to Anna Pasquali and Pierluigi Monaco for fruitful discussions. Finally, we very much appreciate the careful and constructive reading of our paper by the anonymous referee.

REFERENCES

Abadi M. G., Moore B., Bower R. G., 1999, MNRAS, 308, 947
Bahé Y. M., McCarthy I. G., Balogh M. L., Font A. S., 2013, MNRAS, 430, 3017
Balogh M. L., Morris S. L., Yee H. K. C., Carlberg R. G., Ellingson E., 1997, ApJ, 488, L75
Balogh M. L., Navarro J. F., Morris S. L., 2000, ApJ, 540, 113
Balogh M. L., Baldry I. K., Nichol R., Miller C., Bower R., Glazebrook K., 2004, ApJ, 615, L101
Berrier J. C., Stewart K. R., Bullock J. S., Purcell C. W., Barton E. J., Wechsler R. H., 2009, ApJ, 690, 1292
Blanton M. R., Berlind A. A., 2007, ApJ, 664, 791
Blanton M. R., Moustakas J., 2009, ARA&A, 47, 159
Blanton M. R., Roweis S., 2007, AJ, 133, 734
Blumenthal G. R., Faber S. M., Primack J. R., Rees M. J., 1985, Nature, 313, 72
Bower R. G., Benson A. J., Malbon R., Helly J. C., Frenk C. S., Baugh C. M., Cole S., Lacey C. G., 2006, MNRAS, 370, 645
Bower R. G., Benson A. J., Crain R. A., 2012, MNRAS, 422, 2816
Boylan-Kolchin M., Ma C.-P., Quataert E., 2008, MNRAS, 383, 93
Brinchmann J., Charlot S., White S. D. M., Tremonti C., Kauffmann G., Heckman T., Brinkmann J., 2004, MNRAS, 351, 1151
Contini E., De Lucia G., Villalobos Á., Borgani S., 2014, MNRAS, 437, 3787
Croton D. J., 2006, MNRAS, 369, 1808
Cucciati O. et al., 2012, A&A, 548, A108
Daddi E. et al., 2007, ApJ, 670, 156
Davé R., Oppenheimer B. D., Finlator K., 2011, MNRAS, 415, 11
Davis M., Geller M. J., 1976, ApJ, 208, 13
De Lucia G., 2011, Modelling the Evolution of Galaxies as a Function of Environment. Springer-Verlag, Berlin, p. 203
De Lucia G., Blaizot J., 2007, MNRAS, 375, 2
De Lucia G., Weinmann S., Poggianti B. M., Aragón-Salamanca A., Zaritsky D., 2012, MNRAS, 423, 1277
Dekel A., Devor J., Hetzroni G., 2003, MNRAS, 341, 326
Diemand J., Kuhlen M., Madau P., 2007, ApJ, 667, 859
Dressler A., 1980, ApJ, 236, 351
Elbaz D. et al., 2007, A&A, 468, 33
Farouki R., Shapiro S. L., 1981, ApJ, 243, 32
Font A. S. et al., 2008, MNRAS, 389, 1619
Franx M., van Dokkum P. G., Schreiber N. M. F., Wuyts S., Labbé I., Toft S., 2008, ApJ, 688, 770
Geha M., Blanton M. R., Yan R., Tinker J. L., 2012, ApJ, 757, 85
Gunn J. E., Gott J. R., III, 1972, ApJ, 176, 1
Guo Q. et al., 2011, MNRAS, 413, 101
Haas M. R., Schaye J., Jeeson-Daniel A., 2012, MNRAS, 419, 2133
Haines C. P. et al., 2009, ApJ, 704, 126
Henriques B. M. B., White S. D. M., Thomas P. A., Angulo R. E., Guo Q., Lemson G., Springel V., 2013, MNRAS, 431, 3373
Hirschmann M., Naab T., Somerville R. S., Burkert A., Oser L., 2012a, MNRAS, 419, 3200
Hirschmann M., Somerville R. S., Naab T., Burkert A., 2012b, MNRAS, 426, 237
Hirschmann M., De Lucia G., Iovino A., Cucciati O., 2013a, MNRAS, 433, 1479
Hirschmann M. et al., 2013b, MNRAS, 436, 2929
Ilbert O. et al., 2013, A&A, 556, A55
Kang X., van den Bosch F. C., 2008, ApJ, 676, L101
Kauffmann G.et al., 2003, MNRAS, 341, 33
Kauffmann G., White S. D. M., Heckman T. M., Ménard B., Brinchmann J., Charlot S., Tremonti C., Brinkmann J., 2004, MNRAS, 353, 713
Kimm T. et al., 2009, MNRAS, 394, 1131
Knebe A., Libeskind N. I., Knollmann S. R., Martinez-Vaquero L. A., Yepes G., Gottlöber S., Hoffman Y., 2011, MNRAS, 412, 529
Knobel C.et al., 2013, ApJ, 769, 24
Kovač K.et al., 2014, MNRAS, 438, 717
Larson R. B., Tinsley B. M., Caldwell C. N., 1980, ApJ, 237, 692
Ludlow A. D., Navarro J. F., Springel V., Jenkins A., Frenk C. S., Helmi A., 2009, ApJ, 692, 931
McGee S. L., Balogh M. L., Bower R. G., Font A. S., McCarthy I. G., 2009, MNRAS, 400, 937
McGee S. L., Balogh M. L., Wilman D. J., Bower R. G., Mulchaey J. S., Parker L. C., Oemler A., 2011, MNRAS, 413, 996
Mamon G. A., Sanchis T., Salvador-Solé E., Solanes J. M., 2004, A&A, 414, 445
Mok A. et al., 2013, MNRAS, 431, 1090
Mok A. et al., 2014, MNRAS, 438, 3070
Moore B., Lake G., Katz N., 1998, ApJ, 495, 139
Muldrew S. I.et al., 2012, MNRAS, 419, 2670
Oemler A., Jr, 1974, ApJ, 194, 1
Pasquali A., Gallazzi A., Fontanot F., van den Bosch F. C., De Lucia G., Mo H. J., Yang X., 2010, MNRAS, 407, 937
Peebles P. J. E., 1965, ApJ, 142, 1317
Peng Y.-j., Lilly S. J., Renzini A., Carollo M., 2012, ApJ, 757, 4
Planck Collaboration XVI, 2013, preprint (arXiv:1311.1657)
Poggianti B. M., Smail I., Dressler A., Couch W. J., Barger A. J., Butcher H., Ellis R. S., Oemler A., Jr, 1999, ApJ, 518, 576
Rasmussen J., Mulchaey J. S., Bai L., Ponman T. J., Raychaudhury S., Dariush A., 2012, ApJ, 757, 122
Salim S.et al., 2007, ApJS, 173, 267
Skibba R. A., Sheth R. K., 2009, MNRAS, 392, 1080
Somerville R. S., Hopkins P. F., Cox T. J., Robertson B. E., Hernquist L., 2008, MNRAS, 391, 481
Springel V., 2005, MNRAS, 364, 1105
Tal T. et al., 2014, ApJ, 789, 164
Tinker J. L., Wetzel A. R., 2010, ApJ, 719, 88
van den Bosch F. C., Aquino D., Yang X., Mo H. J., Pasquali A., McIntosh D. H., Weinmann S. M., Kang X., 2008, MNRAS, 387, 79
Villalobos Á., De Lucia G., Weinmann S. M., Borgani S., Murante G., 2013, MNRAS, 433, L49
von der Linden A., Wild V., Kauffmann G., White S. D. M., Weinmann S., 2010, MNRAS, 404, 1231
Wang J., De Lucia G., Kitzbichler M. G., White S. D. M., 2008, MNRAS, 384, 1301
Wang L., Weinmann S. M., Neistein E., 2012, MNRAS, 421, 2472
Weinmann S. M., Kauffmann G., van den Bosch F. C., Pasquali A., McIntosh D. H., Mo H., Yang X., Guo Y., 2009, MNRAS, 394, 1213
Weinmann S. M., Kauffmann G., von der Linden A., De Lucia G., 2010, MNRAS, 406, 2249

Downloaded from https://academic.oup.com/mnras/article/444/3/2938/1062092 by CNRS - ISTO user on 25 April 2022

Weinmann S. M., Pasquali A., Oppenheimer B. D., Finlator K., Mendel J. T., Crain R. A., Macciò A. V., 2012, MNRAS, 426, 2797
Wetzel A. R., Tinker J. L., Conroy C., 2012, MNRAS, 424, 232
Wetzel A. R., Tinker J. L., Conroy C., van den Bosch F. C., 2013, MNRAS, 432, 336
Wetzel A. R., Tinker J. L., Conroy C., Bosch F. C. V. D., 2014, MNRAS, 439, 2687
White S. D. M., Rees M. J., 1978, MNRAS, 183, 341
Wilman D. J., Zibetti S., Budavári T., 2010, MNRAS, 406, 1701
Wilson E. B., 1927, J. Am. Stat. Assoc., 22, 209
Woo J. et al., 2013, MNRAS, 428, 3306
Yang X., Mo H. J., van den Bosch F. C., Pasquali A., Li C., Barden M., 2007, ApJ, 671, 153

This paper has been typeset from a TEX/LATEX file prepared by the author.

Downloaded from https://academic.oup.com/mnras/article/444/3/2938/1062092 by CNRS - ISTO user on 25 April 2022